8-2016

Determination of Kinetic Parameters of Equilibrium Peracetic Acid and Hydrogen Peroxide to Calculate Self-Accelerating Decomposition

Ricky Mittiga
Buffalo State College, mittr47@mail.buffalostate.edu

Determination of Kinetic Parameters of Equilibrium Peracetic Acid and

Hydrogen Peroxide to Calculate Self-Accelerating Decomposition

Temperature

By

Ricky Mittiga

An abstract of a thesis
In
Multidisciplinary Studies

Submitted in Partial Fulfillment
Of the requirements
For the degree of

Master of Science

August 2016

Buffalo State College
State University of New York
Department of Chemistry

Abstract of Thesis

Determination of Kinetic Parameters of Equilibrium Peracetic Acid and Hydrogen
Peroxide to Calculate Self-Accelerating Decomposition Temperature

Peracetic acid is a simple molecule that works as a powerful oxidant in
many applications including food safety and water disinfection. The synthesis of
the compound is fairly well understood due to its straightforward synthesis by
mixing acetic acid and hydrogen peroxide. However, the decomposition of the
compound has not been well studied. Few sources are available to provide
kinetic data for the decomposition along with data that shows when the
compound will undergo a self-accelerated decomposition that could lead to
disastrous effects.

This paper demonstrates and discusses an effortless way to determine
kinetic parameters for the decomposition of peracetic acid in equilibrium with
hydrogen peroxide using basic first-order kinetics. Activation energy values were
found to be approximately 70-90 $^{kJ}/_{mol}$ for the various formulations. The enthalpy
of decomposition was determined by differential scanning calorimeter (DSC) and
related to the total active oxygen of the formulation. Once these parameters
were established, the self-accelerating decomposition temperature (SADT) was
determined using the Semenov equation. Final SADT values were determined to
be about 70°C for 225 kg drums and 60°C for 1500 kg containers. This work
applies chemical kinetics to a real world system that is not well understood by its
users.

Buffalo State College
State University of New York
Department of Chemistry

Determination of Kinetic Parameters of Equilibrium Peracetic Acid and Hydrogen Peroxide to Calculate Self-Accelerating Decomposition Temperature

A Thesis in
Chemistry
by

Ricky Mittiga

Submitted in Partial Fulfillment
of the Requirements
for the Degree of

Master of Science
August 2016

Dates of Approval:

_____   _____

Joonyeong Kim, PhD.
Associate Professor of Chemistry
Chairperson of the Committee
Thesis Adviser

_____   _____

M. Scott Goodman, PhD.
Professor and Chair of Chemistry

_____   _____

Kevin Miller, PhD.
Interim Dean of the Graduate School

THESIS COMMITTEE SIGNATORY

Dates of Approval:

_____   _____

                                           Joonyeong Kim, PhD.
                                           Associate Professor of Chemistry

_____   _____

                                           M. Scott Goodman, PhD.
                                           Professor and Chair of Chemistry

_____   _____

                                           Maria Pacheco, PhD.
                                           Associate Professor of Chemistry

Table of Contents   **Page**

List of Symbols

Symbol	Description	Value	Units
q	Heat Generation		J
H	Enthalpy		$J\ kg^{-1}$
V	Volume		m^3
ρ	Density		$kg\ m^{-3}$
A	Pre-exponential Factor		$days^{-1}$
E_a	Activation Energy		$J\ mol^{-1}$
R	Gas Constant	8.314	$J\ K^{-1}\ mol^{-1}$
T	Temperature		K
h	Heat Transfer Coefficient		$W\ m^{-2}\ K^{-1}$
S	Surface Area		m^2
m	Mass		kg
AO	Active Oxygen		%
%RSD	Relative Standard Deviation		
k	Thermal Conductivity		$W\ m^{-1}\ K^{-1}$
x	Wall Thickness		m
$Q^{\neq*}$	Partition Coefficient for Activated Complex		dm
Q_x, Q_{yz}	Partition Function for Reactants		dm
κ	Transmission Coefficient		
h_o	Planck Constant	$6.63*10^{-34}$	$m^2\ kg\ s^{-1}$
k_b	Boltzmann Constant	$1.38*10^{-23}$	$m^2\ kg\ s^2\ K^{-1}$
T_f	Temperature of Fluid		K
T_a	Ambient Temperature		K
T_c	Critical Temperature		K
T_1	Critical Temperature at Tangent		K
MW_{po}	Molecular Weight, Peroxygen		$g\ mol^{-1}$

List of Figures

List of Tables

Chapter 1: Introduction

1.1 Peroxygen Compounds

Inorganic and organic peroxides are tremendously popular in industry and laboratories because of their reactivity and oxidative power. The bonding in this group of chemicals is also valuable as it readily cleaves into highly reactive radicals. The unusual weakness of the O-O bond in peroxygen compounds is what makes these compounds interesting. The instability is associated with the high enthalpy of decomposition, low activation energy, reaction kinetics and structure of the compound. Another factor takes into account the amount of active oxygen (AO) in the formulation [1]. Active oxygen is a term that relates the amount of active species in a formulation. It is a simple ratio of an oxygen atom to the molecular weight of the peroxygen compound, MW_{po}. Equation 1 shows a simplified version of the calculation.

$$AO, \% = \left(\frac{15.99}{MW_{po}}\right) x \; 100 \tag{1}$$

The first man-made organic peroxide was benzoyl peroxide in 1858 [2]. It also became the first commercially available organic peroxide that was used to bleach vegetable oils in the early 1900's. From that point on, more and more peroxides became available commercially for a variety of uses. Figure 1 displays a list of organics that can form organic peroxides. With the increase of peroxygen compound research and synthesis, it was found that some peroxides can become extremely dangerous to handle and even auto-oxidize over time [3].

Heat, mechanical shock, friction, shaking or contamination can cause these compounds to decompose rapidly or possibly explode [4]. Peracetic acid is one of the simplest examples of an organic peroxide.

Structure	Examples
—C(H)—O—	ethers, acetals, secondary alcohols, oxygen heterocycles
>C=C<	olefins with allylic H, terpenes, tetrahydronaphthalene
—CH₂, —CH₂ / C(H)—	isopropyl compounds, decahydronaphthalenes
>C=C—C(H)—	allyl compounds
>C=C(X)(H)	haloalkenes, vinyls
>C=C—C=C< (H H)	dienes
>C=C(H)—C≡C—	vinylacetylenes
—C—C(H)—Ar	cumenes, styrenes
—C(H)=O	aldehydes
—C(=O)—N—C(H)<	N-alkyl amides, ureas, lactams
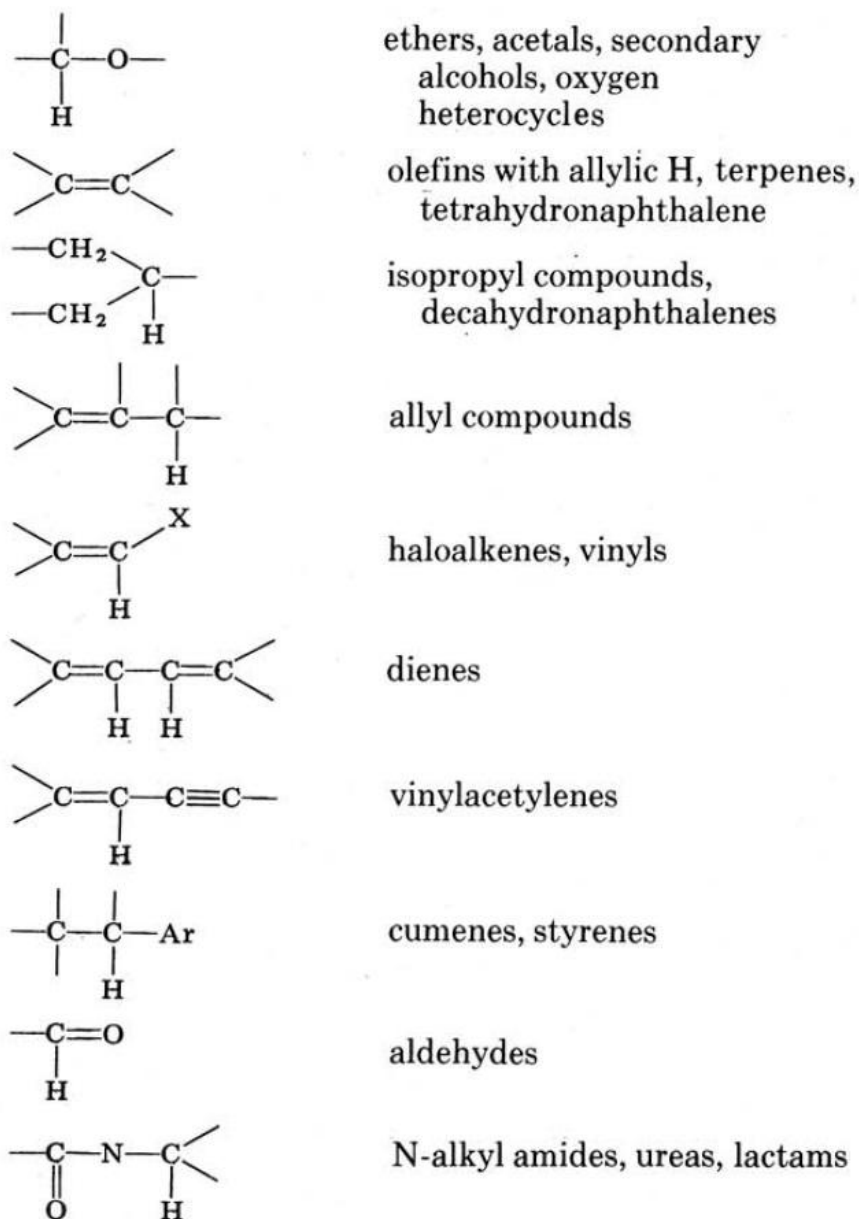
Figure 1: Some organic compounds with structural components that are susceptible to forming peroxide in either air or when combined with hydrogen peroxide. This list if for illustrative purposes and is not definitive [3].

3

1.2 Peracetic Acid

Peracetic acid (PAA), shown in Figure 2, is commonly used as an alternative oxidant to chlorine dioxide because it has a stronger reduction potential of 1.81 V compared to the chlorine dioxide's reduction potential of 1.57 V [5]. PAA has been applied to disinfection of waste water, poultry carcasses, medical equipment and aseptic packaging [6-9]. It can also be used to bleach textiles and pulps or for oxidation of chemical species in chemical manufacturing [10, 11]. There is a growing trend of plants shifting away from chlorine due to its environmental impact and some market pressure to lower price. Because of these factors, PAA is becoming more attractive in industry. In most facilities that already use chlorine the process would only require small changes in equipment to begin using PAA [12]. This is a huge advantage since it would be difficult for most plants to make large changes to an existing process in order to use a new disinfectant.

PAA is commonly synthesized by the reaction of acetic acid with hydrogen peroxide, sometimes in the presence of a catalyst. Other ways of creating the compound include the oxidation of acetaldehyde or the reaction of acetic anhydride with hydrogen peroxide. However, the acetic anhydride production method can create diacetyl peroxide, which is extremely unstable [13]. The reactions of acetic acid or acetic anhydride with hydrogen peroxide proceed to an equilibrium mixture of the reactants and products as shown in Eq. (2) and (3).

$$CH_3COOH + H_2O_2 \xrightleftharpoons{Catalyst} CH_3COOOH + H_2O \qquad (2)$$
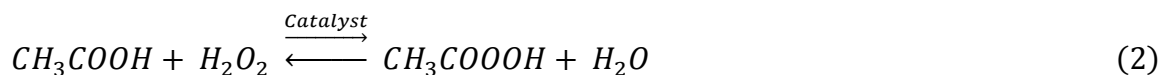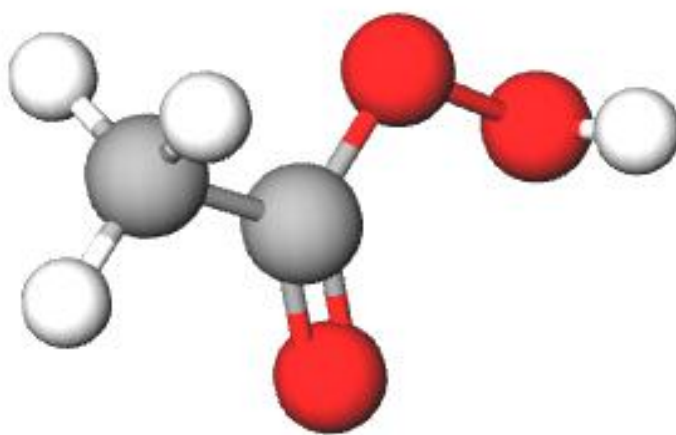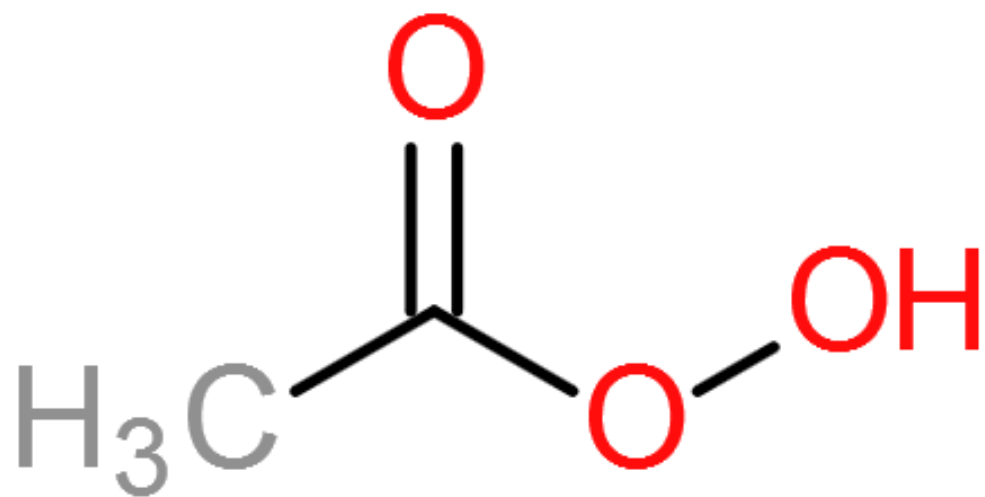
Figure 2: 2-D and 3-D Representation of a PAA molecule.

$$CH_3COOOCCH_3 + 2H_2O_2 \underset{\longleftarrow}{\overset{Catalyst}{\longrightarrow}} 2CH_3COOOH + H_2O \tag{3}$$
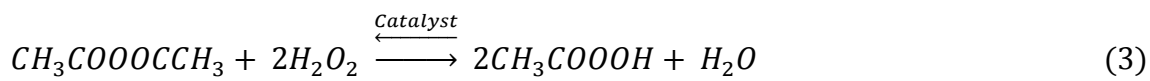
The reaction in Eq. (2) is preferred because it is an easier process to design with the monitoring needed to control the reaction. There are also no side reactions that can create dangerous byproducts like diacetyl peroxide.

With the popularity of PAA increasing due to its ease of production and the environmentally friendly byproducts that are created from its decomposition, there has been an increasing demand for the material that is difficult to meet without the ability to ship and store the compound in large quantities (greater than 330 gallons). This is problematic since most peroxygen compounds are inherently thermally unstable. When PAA decomposition occurs, the reaction typically follows the routes shown in the following three reactions (Eq. 4-6):

$$Hydrolysis: CH_3COOOH + H_2O \rightarrow CH_3COOH + H_2O_2 \tag{4}$$

$$Spontaneous\ Decomposition: 2CH_3COOOH \rightarrow 2CH_3COOH + O_2 \tag{5}$$
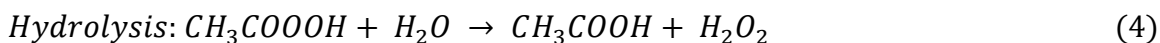
$Transition\ Metal\ Catalyzed:$

$$2CH_3COOOH \xrightarrow{Metal\ Ion} 2CH_3COOH + O_2 + other\ products \tag{6}$$
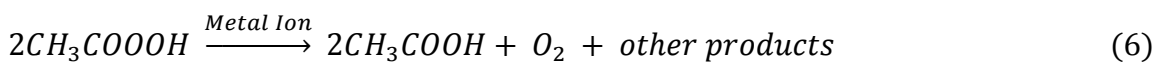
When PAA decomposes, pressure will build in a container since oxygen is being generated in most of the above equations. Therefore, appropriate engineering of containers is essential for PAA storage. Containers must be built with pressure relief to prevent pressure build-up caused by accumulating oxygen gas. Safe containment can turn into a serious problem if a pressure relief device is

defective, blocked or if decomposition is so severe that it overwhelms the capacity of safety devices.

The equilibrium of PAA is complex and makes hydrolysis difficult to track. The decomposition is driven by the hydrolysis of PAA since it is the least stable of the components. Since this decomposition leads to the formation of the reactants, PAA can be continually reformed. At room temperature, hydrogen peroxide is very stable, so the lowering of the assay of PAA and hydrogen peroxide is related to spontaneous decomposition of PAA. The hydrogen peroxide assay decreases over time because of the reformation of PAA due to the increase in acetic acid from the decomposition reactions. Due to this equilibrium shift to the left, PAA needs to be formed to maintain the equilibrium.

At ambient temperatures, hydrolysis and spontaneous decomposition generally occur slowly, with hydrolysis being more important than spontaneous decomposition [12]. The metal ion catalyzed decomposition will be significantly faster at lower temperatures than hydrolysis [14]. Metal ion concentrations as low as 10-20 ppm can initiate the reaction, and the typical metal ions of concern are iron, cobalt, manganese and copper in the divalent oxidation state. These ions can initiate what is called Fenton's reaction. These conditions allow the metal ion to transition from both a high and low valency because the peroxide can act as an oxidizer and reducer [15]. An example of a Fenton's reaction scenario would involve contamination with iron. The reactions below show how iron becomes oxidized and reduced due to the production of different radicals of hydrogen peroxide [16].

$$Fe^{2+} + H_2O_2 \rightarrow Fe^{3+} + OH^- + OH^{\cdot} \tag{7}$$

$$OH^{\cdot} + H_2O_2 \rightarrow HO_2^{\cdot} + H_2O \tag{8}$$

$$Fe^{3+} + HO_2^{\cdot} \rightarrow Fe^{2+} + H^+ + O_2 \tag{9}$$

$$Fe^{2+} + HO_2^{\cdot} \rightarrow Fe^{3+} + HO_2^- \tag{10}$$

Several methods have been employed that help minimize the impact of metal impurities. These methods include passivating metal containers [17], using sequestering agents [18], or adding inorganic salts [19].

Another safety concern around PAA would be a self-heating event. This situation occurs when the external temperature is high enough to heat the product to a critical temperature. The heat generated from the solution cannot be dissipated into the environment as quickly as it is produced [20]. This critical temperature is called the self accelerating decomposition temperature (SADT) and is a main concern for transportation and storage since most trucks and warehouses are not refrigerated. It is easier to prevent metal contamination, which can lower the SADT value, than it is to keep significant amounts of PAA refrigerated at a low temperature. Most of the focus of new PAA formulations is to increase this SADT value.

1.3 Calculation of SADT

One of the first mathematical representations of the critical conditions relating the size and shape of the reacting material to its decomposition kinetics was made by Nikolai Semenov in 1928. This equation was derived from the

application of Newton's Law of Cooling, which shows a linear dependence of the cooling rate with excess temperature.

The rate of heat production of the mixture will occur uniformly throughout the mixture to a temperature that is greater than its surroundings. This equation will take into account the enthalpy of decomposition, ΔH, along with Arrhenius kinetic parameters: activation energy, E_a, and pre-exponential factor, A. This equation is given as:

$$q_1 = \Delta H V A e^{\left(-\frac{E_a}{RT_f}\right)} \tag{11}$$

This is assuming that the temperature of the fluid, T_f, is in the early stages of its self-heating and the heat generation is related to the whole volume, V. The next part of the equation takes into account the previously stated Newton's Law of Cooling.

$$q_2 = hS(T_f - T_a) \tag{12}$$

The cooling of the system is the heat transferred from the whole fluid surface in contact with the atmosphere, S, across the container wall and into the surrounding atmosphere. The heat transfer coefficient, (h), of the container wall is dependent on the material that it is constructed of. Some examples are metal, plastic and glass. The values for each material based on its thickness can be easily found in tables.

The critical temperature is determined by setting Eq. (11) and (12) equal to one another along with the first derivative over temperature. These two lines will create a curve and a tangent line that will cross the x-axis that will define the SADT temperature. This is a point where the heat generation of the system is

equal to the loss to the outside. Figure 3 shows a graphical representation of how these lines tangent. This steady state is difficult to reach experimentally for a few reasons. For example, the heat generation of the system is exponential while the heat loss is linear. This shows that under normal circumstances heat will be accumulating in the system faster than it can be removed after a certain point in time depending on the stored chemical energy of the compound. Another issue that is not taken into account is the consumption of the reactant over the course of the decomposition. This loss of active oxygen will cause the temperature increase to slow since the reaction rate will decrease as reactant is consumed [21].

There are situations where the heat loss curve can shift leading to curves that have multiple points of intersection or no intersection at all.   Figure 4 shows graphically how this system would be like in the real world. When the ambient temperature is low, the system is in a stable state where the cooling would out-pace the heat generation of the container. If that ambient temperature were to be increased, it would be more difficult for the system to displace heat that is accumulating and could result in an over-heating leading to ignition. Figure 5 shows how reducing the heat loss could result in the two curves not intersecting which would result in a scenario where ignition would always occur. This would happen if the packaging material became insulated or otherwise changed in a way that prevented proper heat loss out of the system. This would lead to adiabatic conditions within the system.
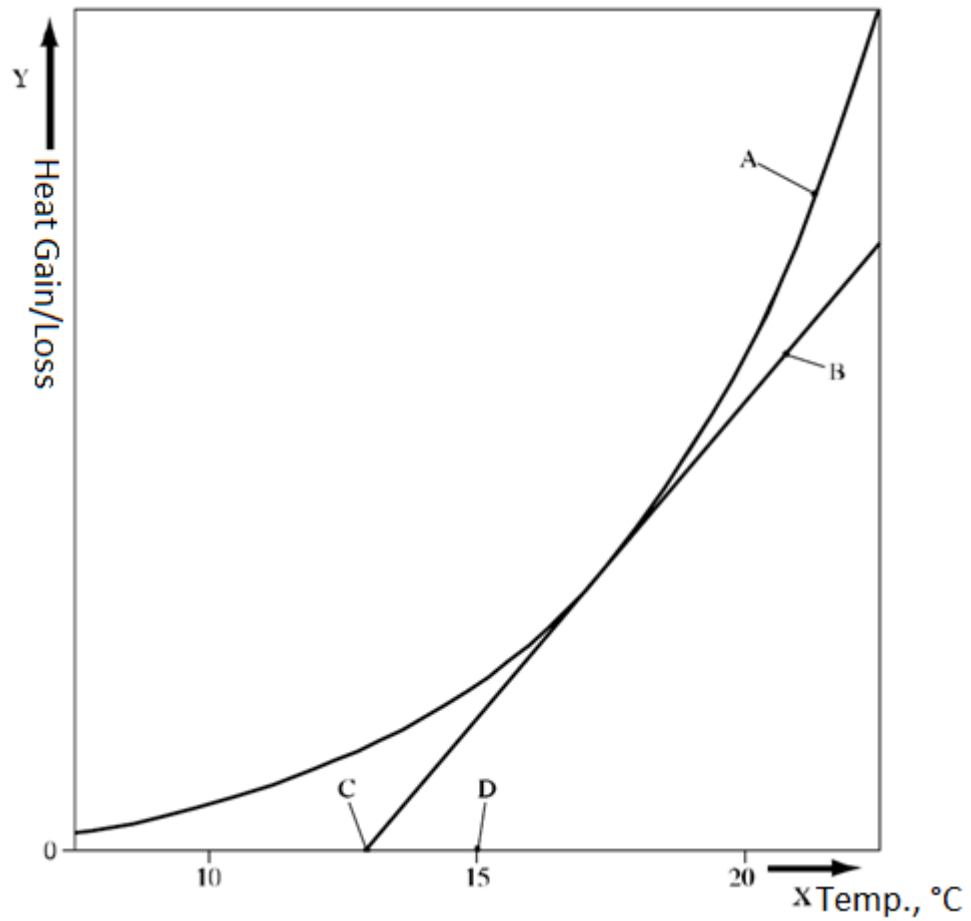
Figure 3: Simplistic graphical representation of the Semenov equation. This image shows that heat generation curve (A) meeting a tangential line (B) at a single point represented as the critical temperature. When the tangent intersects the x-axis at point (C), this represents the actual SADT of the system. Point (D) represents the value that is rounded up to the nearest 5°C and reported.
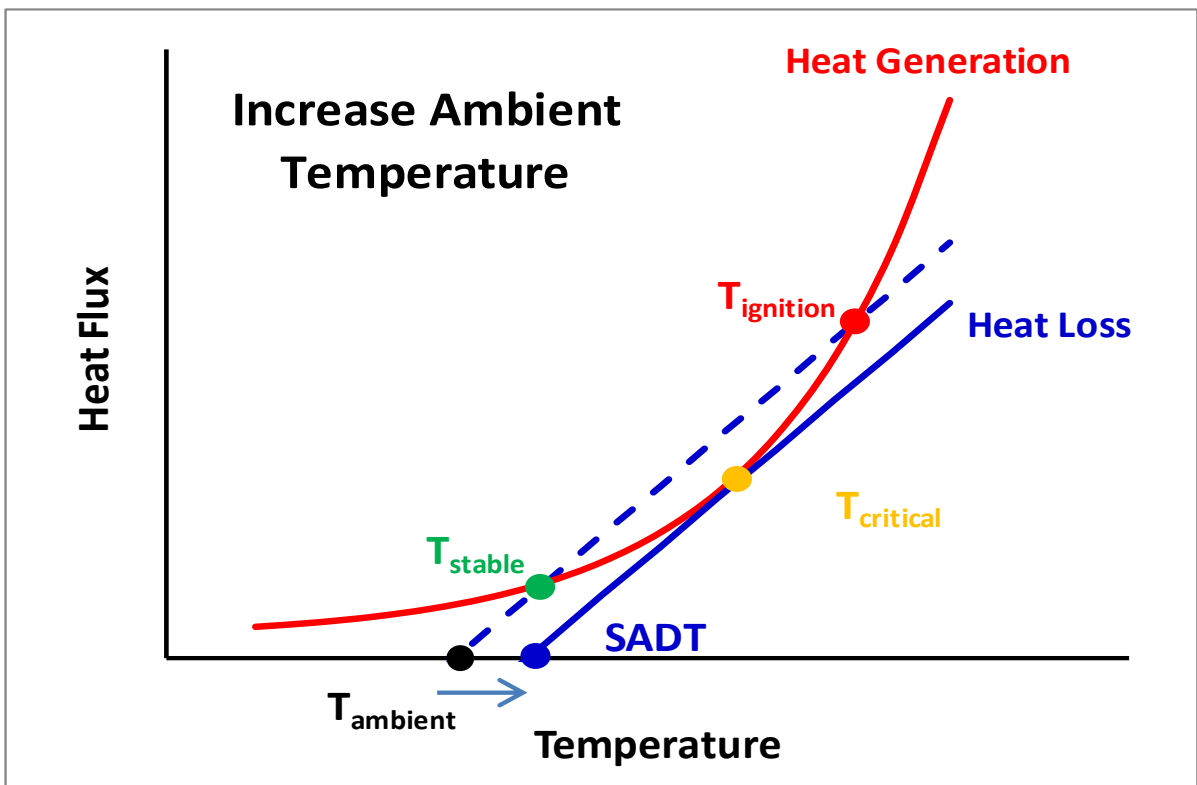
Figure 4: Another representation of the Semenov equation that would represent a real-world situation. The dotted line represents an initial ambient temperature that is low enough to create a region that can keep the system stable. If the ambient temperature is increased, the chart shows how the critical point is reached and the SADT is extrapolated.
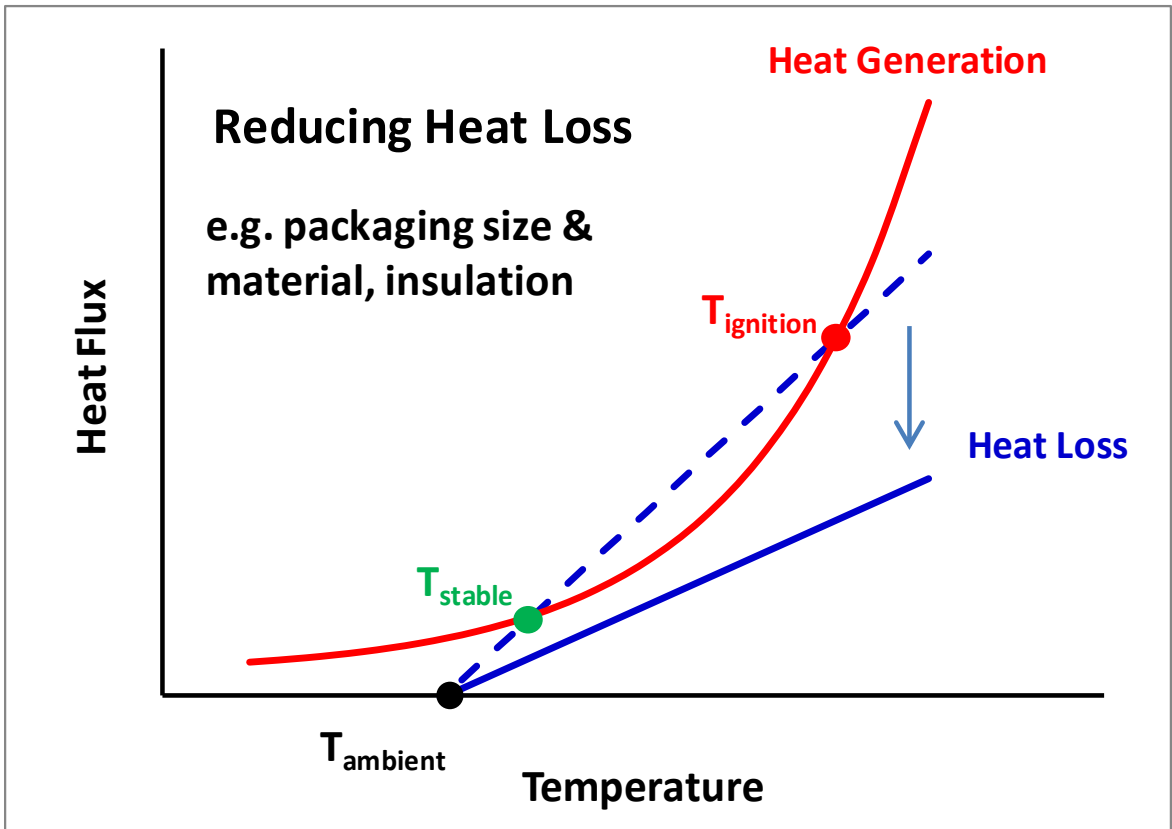
Figure 5: This represents a situation where the heat loss in the system is reduced leading to adiabatic conditions within the container. This shows that all situations lead to ignition because the heat generation is always greater than the heat loss.

Setting Eq. (11) and (12) to be equal to one another and rearranging the terms an equation that allows for the calculation of the SADT can be obtained using Eq. (13). Since the SADT value is used on both sides of the equation, it needs to be solved using an iterative approach. Iteration involves recalculating a result based on an initial guess and finally converging on a final result based on a certain termination criteria. In this case, the termination criterion is when both sides of the equation are equal.

$$T_{SADT} = \sqrt{\frac{mHE_a}{hSR} * \frac{A}{24} * e^{(1-\frac{-E_a}{RT_{SADT}})}} \tag{13}$$

1.4 Derivation of the SADT Equation

The derivation of the workable Semenov equation is quite complicated and requires the ability to make some approximations, within reason [22]. Initially, it is necessary to relate q_1 and q_2 at the point of tangency where the fluid temperature is equal to the critical temperature. This will relate T_f with the temperature at which the heat loss and heat generation curve intersect at T_1. In addition, the atmospheric temperature, T_a, will be converted to the critical temperature, T_c, at which the heat generation of the system begins to run away.

$$\Delta HAVe^{(\frac{-E_a}{RT_1})} = hS(T_1 - T_c) \tag{14}$$

Next, setting the conditions of the derivatives with respect to temperature of dq_1/dT and dq_2/dT equal to one another.

$$\frac{\Delta HAEV}{RT_1^2} e^{(\frac{-E_a}{RT_1})} = hS \tag{15}$$

14

Substituting Eq. (14) into Eq. (15) provides a quadratic with respect to T_1

$$\frac{RT_1^2}{E} - T_1 + T_c = 0 \tag{16}$$

Solving the quadratic for T_1 yields

$$T_1 = \frac{1 \pm \sqrt{1 - 4\frac{R}{E}T_c}}{2\frac{R}{E}} \tag{17}$$

A rough approximation with $4RT_c/E$ is then taken using a T_c of 350 K and an E of 40 kcal/mole, which are fairly representative values of sensitive compounds. This results in a value of about 0.07 meaning that the term should not be approximated as 1. We will move to determine the positive root of Eq. (17).

$$T_1 = \frac{E}{2R}\left[1 + \left(1 - 4\frac{R}{E}T_c\right)^{\frac{1}{2}}\right] \cong \frac{E}{2R}\left(2 - 2\frac{R}{E}T_c\right) = \frac{E}{R} - T_c \tag{18}$$

Using the same approximations from Eq. (17), a value for T_1 is given as 20,000 K which is unrealistic making this root not a good option to use. The next step would then move to the negative sign of Eq. (17).

$$T_1 = \frac{E}{2R}\left[1 - \left(1 - 4\frac{R}{E}\right)^{\frac{1}{2}}\right] \cong \frac{E}{2R} * \frac{R}{E}T_c = T_c \tag{19}$$

Eq. (19) shows how the relation of the T_1 is related to the critical temperature of the system. If we expand the square root from Eq. (17) as a series, we obtain

$$T_1 = \frac{E}{2R}\left[2\left(\frac{RT_c}{E}\right) + 2\left(\frac{RT_c}{E}\right)^2 + \cdots\right]$$ (20)

Eq. (20) will then reduce down to

$$T_1 \cong T_c + \frac{RT_c^2}{E}$$ (21)

The pre-explosion rise will relate to ΔT_c to be expressed as

$$\Delta T_c = T_1 - T_c = \frac{RT_c^2}{E}$$ (22)

Divide both sides of Eq. (22) by T_c to get

$$\frac{\Delta T_c}{T_c} = \frac{T_1}{T_c} - 1 = \frac{RT_c}{E}$$ (23)

In this case, $\Delta T_c / T_c$ is far less than unity since we show in Eq. (19) that T_1 is relatively equal to T_c. For Eq. (23) to make sense, the term $\Delta T_c / T_c$ generally is valued at 0.01 to 0.02. We then can rearrange Eq. (22) as follows

$$\frac{1}{T_1} = \frac{1}{T_c + \Delta T_c} = \frac{1}{T_c\left(1 + \frac{\Delta T_c}{T_c}\right)}$$ (24)

As stated earlier, since $\Delta T_c / T_c$ is far less than unity, Eq. (16) can be changed to reflect that

$$\frac{1}{T_1} \cong \frac{1}{T_c}\left(1 - \frac{\Delta T_c}{T_c}\right)$$ (25)

With all this information, we can substitute Eq. (22), (23) and (25) into Eq. (14) to remove T_1 to obtain

16

$$\frac{\Delta HAEV}{hSRT_c^2} e^{(1-\frac{E_a}{RT_c})} = 1 \qquad (26)$$

In this case, T_c is the SADT temperature of the system. Multiplying both sides of Eq. (26) by T_c^2 will result in Eq. (13) [22].

1.5 Current Methodologies to Determine SADT

According to the Recommendations on the Transportation of Dangerous Goods, there are a few acceptable methods to determine SADT that fall under section 28, test series H [23]. Each test follows the same general test guidelines for storing the chemical at a preset external temperature and observing for any chemical reaction or heat generation at near adiabatic conditions. These are all based off the Semenov explosion model calculation. The rate of heat generation within the product is measured and plotted against the isothermal temperature at which the test was conducted for the determination of the SADT value. There are some differences for each test that allow flexibility for the testing of large quantities of sample or different types of compounds. These compounds include solids, liquids, pastes and dispersions.

One of the ways of conducting the test is with an adiabatic test chamber that is well insulated, has the ability to maintain air temperature +/- 2°C and is big enough to maintain at least a 100 mm distance from the package and the wall of the chamber. Figure 6 shows a schematic of an adiabatic chamber for a small package up to 25L. The benefit of this system is the test only needs to be run once to get an accurate SADT value. Once exothermic activity is detected by the

instrument, this self-heating is tracked until this activity ceases. This could extend on for several days. Once the peak value is determined, the test is terminated and the self-heating rate along with the power output at various temperatures is determined. These values are used to generate a heat generation curve that can be used to determine the SADT values. An example of the heat generation profile is shown in Figure 7.

The linear equation derived from this heat generation profile helps to determine the SADT value by providing the heat generation at any given temperature. Since the heat loss curve is known, the tangential point can be determined and the SADT value is determined. Kinetic parameters can be obtained from the linear equation. Initially, it starts out with Eq. (27),

$$y = -15.784x + 45.648 \tag{27}$$

This equation using the axis as a guide can be rewritten as follows,

$$Ln(q) = \left(\frac{-15784}{T}\right) + 45.648 \tag{28}$$

Next, we want to remove the natural log to put the equation into the classic form of the Arrhenius equation,

$$(q) = e^{\left(\frac{-15784}{T}+45.648\right)} \tag{29}$$

Finally, removing the constant from the exponent and bringing it out front,

$$(q) = 6.68 * 10^{19} \, e^{\left(\frac{-15784}{T}\right)} \tag{30}$$

This equation provides a value of 6.68×10^{19} $K/_s$ and the activation energy is 131 $kJ/_{mol}$.

An issue with this method is the possibility of a large explosion with extremely thermal sensitive compounds. This can be overcome with sufficient safety protocols that include a cooling system along with the selection of an appropriate testing site with sufficient space in the event of an explosion.
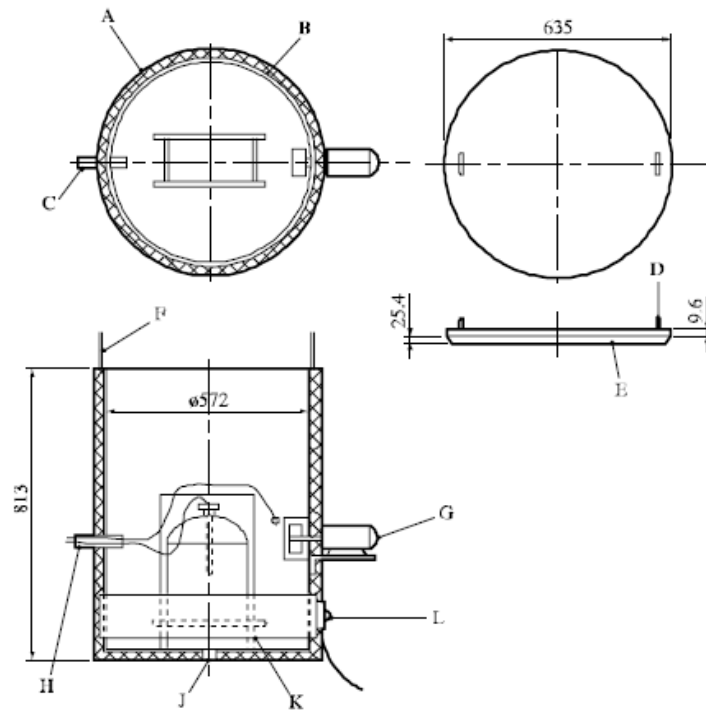
(A) Insulation 25 mm thick   (B)   220 litres open top drum
(C) 19 mm pipe   (D)   9.6 mm eye bolt in steel cover
(E) Insulation on steel cover   (F)   3 mm control cable
(G) Fan   (H)   Thermocouples and controls
(J) Drain   (K)   25 mm angle stand
(L) 2 kW drum heater

Figure 6: Diagram of SADT test apparatus for containers up to 25L. Image from UN Transport of Dangerous Goods [23].
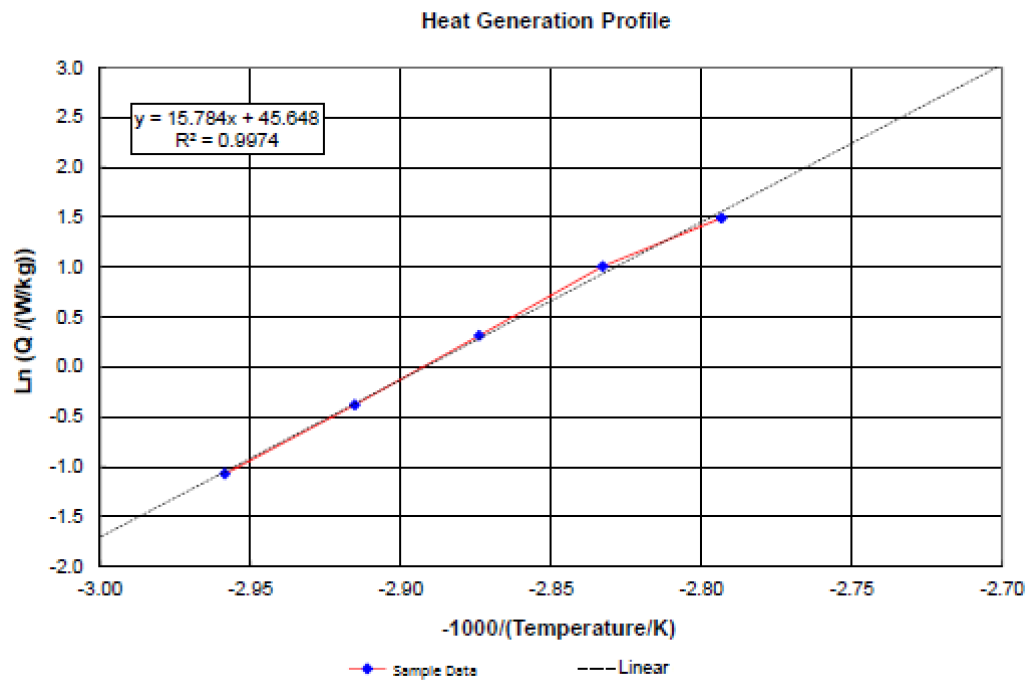
Figure 7: Heat generation profile of an equilibrium PAA sample. Kinetic parameters can be obtained from this starting with Eq. (26). The parameters are then applied to the Semenov equation.

Another method that is used is an isothermal test system that uses very small sample sizes in the range of a few milligrams up to several grams. This eliminates the chance of extreme thermal hazards. This test scheme, shown in Figure 8, uses a dual channel setup; one to record a sample signal and the other that is measuring the blank signal for comparison. This method is more labor intensive since the test should be run for 36 hours and replicated at least 7 times to get results that can vary in heat generation from 15 to 1500 $^{mW}/_{kg}$. This is necessary because these results are then plotted as temperature vs. temperature rise rate. Figure 9 shows the curve that is developed using this type of isothermal technique. This curve only used 3 data points to extrapolate the necessary data to determine the final SADT. The regression curve data found in the figure represents the pre-exponential factor and the activation energy data that is needed to plug into the Semenov equation. The pre-exponential factor in this case is 8.4 x 10^{12} $^{\circ C}/_{min}$ and the exponent is the activation energy divided by the gas constant. For this case, the activation is found to be 98,360 $^{J}/_{mol}$. This method may also be a little more prone to error since separate samples need to be run each time, which increases the risk of a sample being exposed to outside contaminants and may skew the SADT value.
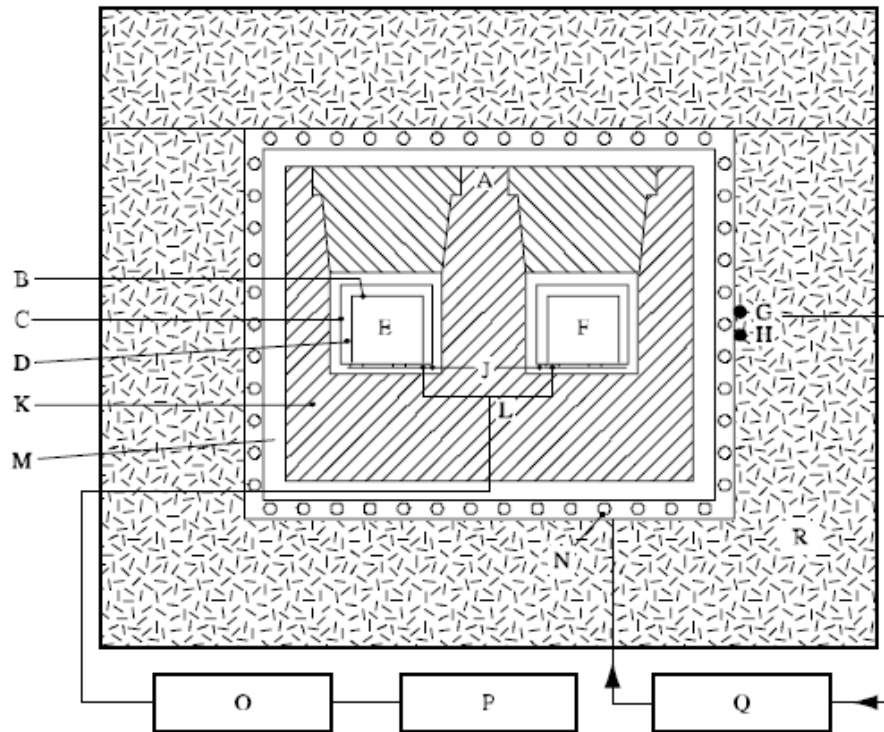
(A) Platinum resistance thermometer   (B) Sample vessel
(C) Cylindrical holder   (D) Air spaces
(E) Sample   (F) Inert material
(G) Platinum resistance sensor   (H) Platinum resistance sensor
    for temperature control   for safety control
(J) Peltier elements   (K) Aluminium block
(L) Electric circuit   (M) Air space
(N) Heating wires   (O) Amplifier
(P) Recorder   (Q) Temperature controller
(R) Glass wool

Figure 8: Diagram for Isothermal Storage Test. Image from the Transport of Dangerous Goods [20].
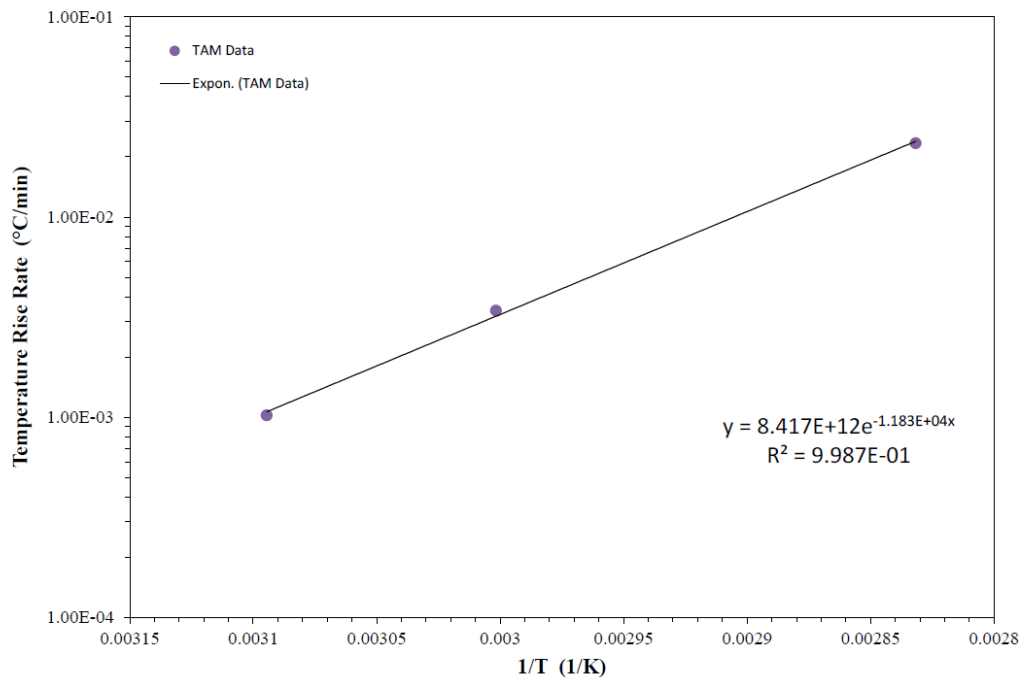
Figure 9: Graphical representation of Thermal Activity Monitor data from outside lab. Kinetic parameters can be derived from the linear equation that is then applied to the Semenov equation.

1.6 Determination of Critical Parameters for SADT Calculation

The idea of activation energy was introduced by Svante Arrhenius in 1889 [24]. The activation energy of the reaction is the minimum energy required for a reaction to occur. This amount of energy can be varied with the addition of a catalyst or stabilizer in the case of this experiment. Temperature variation is the important factor when it comes to self-accelerating decomposition. In this case, peracetic acid is stable at room temperature but when the temperature is increased, the possibility of decomposition is increased. The activation energy is determined experimentally along with the pre-exponential factor from a simple linear equation. Table 1 shows some typical activation energy values for a variety of organic peroxides.

The pre-exponential factor, A, is dependent on how often the molecules collide to produce a reaction. This value can be calculated rather than defined experimentally as the collision frequency factor, designated by a Z, but can differ from experimental values by factors of 10 [25]. Only collisions that have sufficient energy greater than the activation energy will cause a reaction to proceed, but they also have to collide in the proper orientation. This orientation factor is why the calculated value, Z, is sometimes much different than the experimental value, A.

Table 1: Example Enthalpies of Decomposition and Energy of Activation for Various Organic Peroxides.

Organic Peroxide	Structure	ΔH, J/g	Ea, kJ/mol	ΔH, J/g	Ea, kJ/mol	ΔH, J/g	Ea, kJ/mol	ΔH, J/g	Ea, kJ/mol
Benzoyl peroxide	$C_{14}H_{10}O_4$	1834	145					1000	188
t-Butyl hydroperoxide	$C_4H_{10}O_2$	1055	139	3104	114			1600	
Cumene hydroperoxide	$C_9H_{12}O_2$	1876	176	3568	132			1500	
Dilauroyl peroxide	$C_{24}H_{46}O_4$	971	135	588[31]	100[31]			576	
Di-tert-butyl peroxide	$C_8H_{18}O_2$	557	161	2020	111	1211	125	1200	80
Methylethylketone peroxide	$C_8H_{18}O_6$	1444	141					1200	110
Diamyl peroxide	$C_{10}H_{22}O_2$					925	146		
Dicumyl peroxide	$C_{18}H_{22}O_2$					811	130	700	
t-butyl cumyl peroxide	$C_{13}H_{20}O_2$					991	136		
Hydrogen peroxide [29]	H_2O_2	963	336						
Reference		[26]		[27]		[28]		[30]	

1.7 Kinetic Theory of Chemical Reactions

There are two theories that deal with reactions in the liquid phase: Collision and Transition State. These reactions are fundamentally the same in the liquid phase as in the gas phase. However, in solution the interaction of the solvent and the reactants must be taken into account because the changing configurations of the reactants will be influenced by the solvent. The properties of permittivity, viscosity and the polarizability of the solvent will play an important role in these reactions.

The collision theory is the most basic theory and comes down to collision between the reactant molecules with sufficient energy to cause a reaction. Arrhenius explained that molecules must have sufficient kinetic energy to overcome repulsive and bonding forces of the reactants to create products; this is known as the activation energy, E_a. Depending on the amount of energy required, atoms or molecules may collide and simply bounce off one another [32]. Another important detail about collision theory is that the energy that is associated with the reactant atoms or molecules mutual approach is the only energy used to calculate the collision energy. The molecules may also have velocity and momentum in a different direction but that is not accounted for when looking at the energy required to overcome the activation barrier.

The main theory that is utilized in this study is the transition state theory. This is heavily relied upon when it comes to reactions in solutions. Since it is difficult to take into account the charge on the reactants, relative permittivity and change in the solvation pattern, the thermodynamic formulation is used [33]. Collision

theory notes that not all reactions will create products. The transition state theory tells us that there are two possible outcomes from a collision: either they will return to reactants or the molecules will rearrange and create products [34]. When we return to the idea of reactions in solutions, we need to take into account the concept of ideal and non-ideal. The terms are somewhat self-explanatory since ideal solutions behave in a way that is easy to predict and follows theory. Solution based reactions are mainly considered non-ideal. When the solute concentration rises, the solute-solute interaction becomes particularly important, especially if particles or molecular charges are involved.

It was postulated in a paper by Zhao *et al*. [13], that a molecule of PAA has an activated carbonyl that gets attacked by the oxygen in the hydroxyl group of another PAA molecule creating an active intermediary proposed in Figure 10. This intermediary then quickly decomposes into two acetic acid molecules and oxygen. This compound is formed because there is sufficient energy in the system to create this activated complex.

The experiments that are discussed in this paper are done in solutions that have the same general solvent concentration, permittivity and viscosity. Because these factors remain constant throughout the study, the Arrhenius equation can be used and non-ideality does not have to be considered since it is expected to be constant.
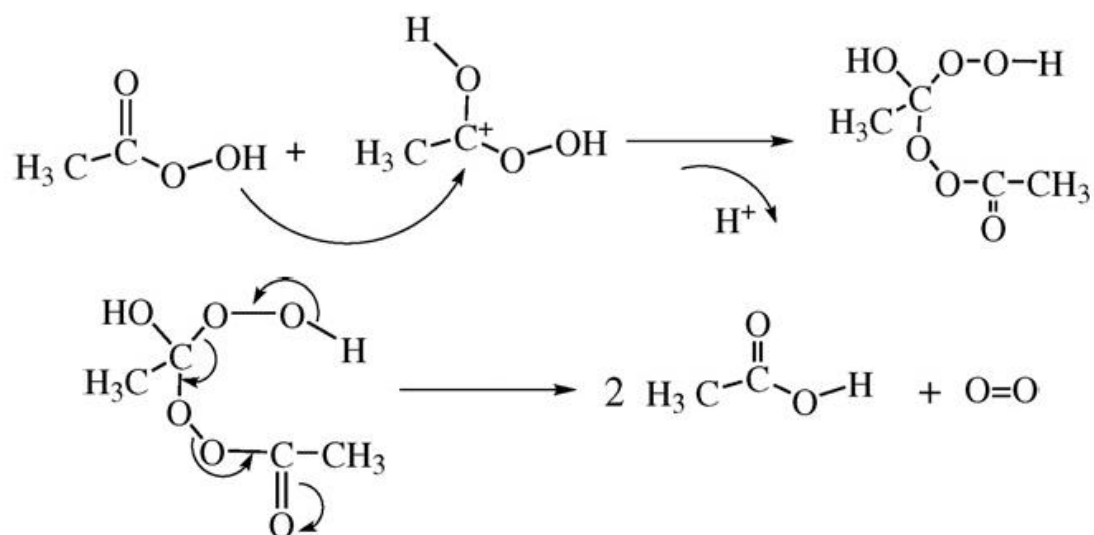
Figure 10: Proposed mechanism of an active intermediary formed with a positively charged carbonyl. This gets attacked by an oxygen atom in the hydroxyl group of another PAA molecule. This rapidly decomposes to acetic acid and a molecule of oxygen.

1.8 Overview of Auto-Titrator

Titrations are one of the most widely used techniques in chemical analysis with very high accuracy and precision. This technique also allows a high degree of automation due to the types of endpoint detection. The indication methods that are available are: pH, potentiometric, voltametric, ampometric, photometric, conductivity and thermometric. The titrator used, shown in Figure 11, used potentiometric and pH titrations to conduct the experiments mentioned throughout.

1.9 Overview of Differential Scanning Calorimeter

A differential scanning calorimeter (DSC), shown in Figure 12, is an instrument that measures the differences in heat flows between a sample and a reference material/sample relative to temperature or time. The reference sample is typically an empty crucible that is placed on the heating element alongside the sample being tested in the same compartment. The differences in heat flow arise from a phase change in the sample. These changes can be due to melting, crystallization, chemical reactions, vaporization or other physical changes [35]. The added benefit of this instrument is that it allows a milligram scale sized sample to be heated at varying temperature rates. This allows samples to be tested quickly. These small sample sizes allow the decomposition onset and enthalpy to be determined with no risk of explosion [36]. The sample size does pose a problem since it is important to obtain a sample that is representative of the bulk solution and measurement errors can add to the variability of the results.

There is also a need for a balance that will accurately measure the small

quantities required [37].
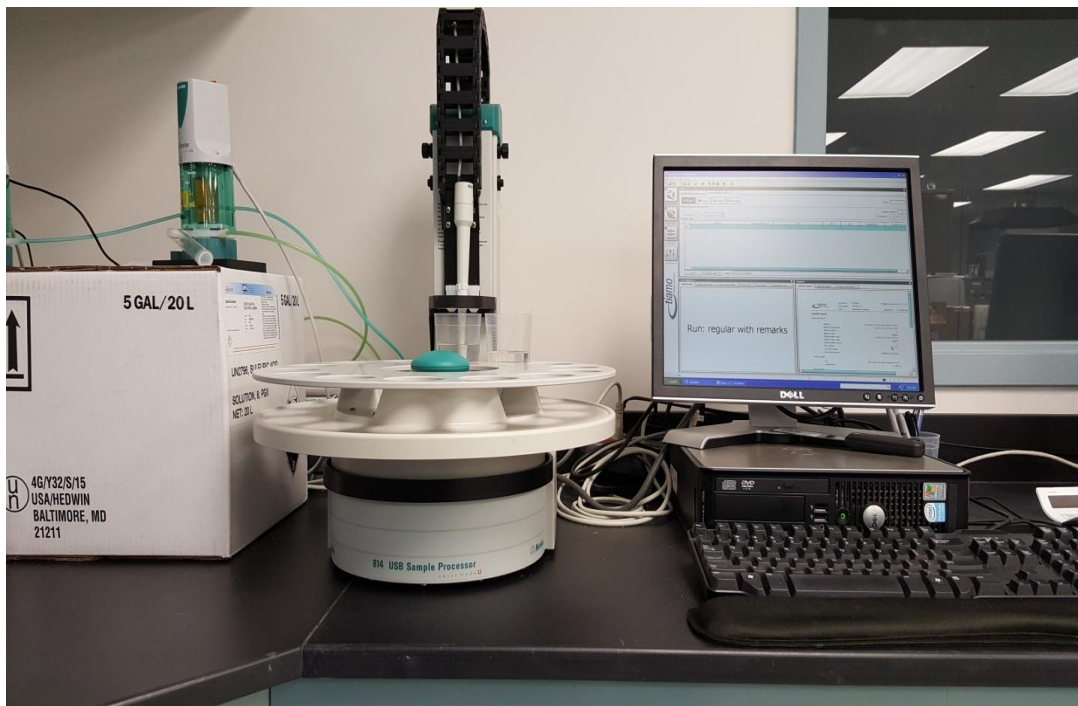
Figure 11: Image of the auto-titrator used in this experiment
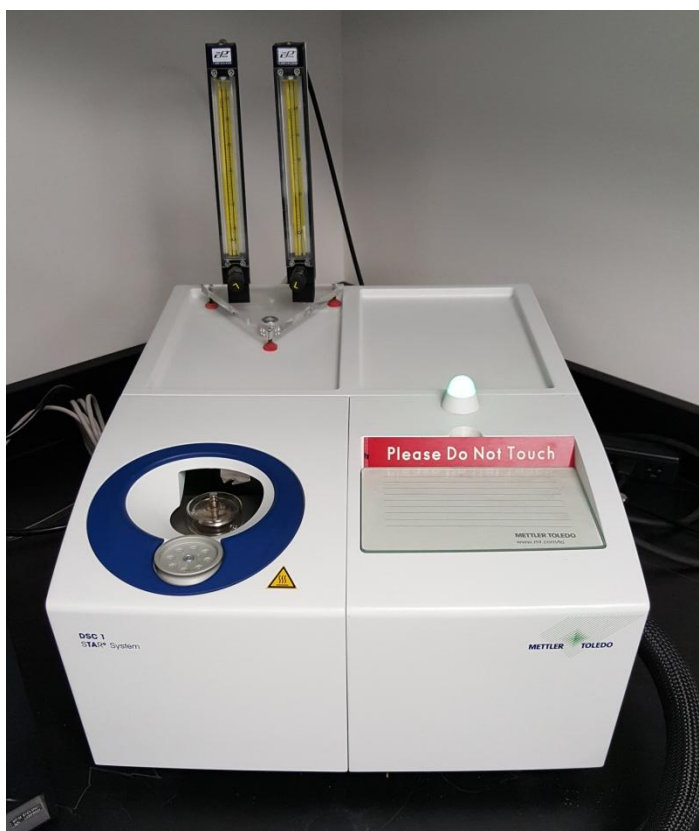
Figure 12: Image of a Mettler-Toledo DSC1.

1.10   Other Critical Factors

The surface area and volume calculations are based on typical calculations for regular shapes of cubes and cylinders. These calculations are important in the final calculation for the SADT because they play a role in the heat transfer to the surrounding environment. The more surface area that is available will allow more of the chemical to have access to the package wall to give off heat. Also, not all surfaces on a container will have the opportunity to contribute to the heat dissipation. For example, a cubic tote that is placed on the floor will not be able to displace heat out the bottom as efficiently as the sides. This leads to an uneven heat dissipation. For the sake of this study, a conservative surface area will be used by calculating the surface area of a sphere with the same volume. There is a delicate balance to maintain in order to achieve a good equilibrium. Even if the container has a large wall surface, the distance from the middle of the container to the wall of the container cannot be too large. Center-to-wall distance is equally important for the heat dissipation.

The heat transfer coefficient, h, depends on the type of material that the chemical is packaged in and the driving force for the flow of heat. The main types of packaging that would be of use in this case are glass, metal and plastic. Each material will have its own value and will vary based on thickness. The simplest form of the heat transfer coefficient is defined as:

$$h = \frac{k}{x} \tag{31}$$

where k is the thermal conductivity of the container material and x is the wall thickness. In the case of SADT values, we have to assume that there is *no*

forced cooling along the surface of the container and that there is *no flow inside the container other than naturally occurring convection* as the solution heats. When the heat transfer coefficient and surface are combined, this implies an effective heat transfer over the surface of the container.

The heat transfer coefficient will be looked up in reference material rather than experimentally determined in this test. This value is not large enough to cause significant changes in the final calculation so general values for most types of material can be used. This coefficient will also take into account the surface area of the package that is able to dissipate heat. Generally, all sides of a container are able to remove heat but it is important to look at real scenarios. In reality, the top and bottom of the container may not remove as much heat as the sides due to storage conditions leaving the sides to remove most of the heat. These factors will be taken into account to determine a conservative estimate of the heat transfer.

1.11   Objectives of the Thesis Project

The purpose of the project is to use the Semenov equation to predict the SADT of an aqueous peracetic acid and hydrogen peroxide mixture existing in equilibrium. It is important that this method calculates values comparable to outside labs so it can be used as a tool to determine the value of new formulations. The first challenge will be to test samples by titration to determine the change in peracetic acid and hydrogen peroxide concentration over time at various temperatures. The overall change in active oxygen will be calculated and will be plotted using the first-order rate expression so each temperature can

provide its own rate. Secondly, each different decomposition rate will be plotted

using the Arrhenius equation. The activation energy and the pre-exponential

factor can be extrapolated from the linear equation.

Chapter 2: Experimental Parameters

2.1 Materials

Samples were prepared using deionized water with a resistivity of at least 18 megohm·cm using an Aries High Purity Water System (Model ARS-102). Glacial acetic acid (> 99.7%, Eastman Chemical), hydrogen peroxide (> 50%, PeroxyChem), etidronic acid (> 60%, Riverside Chemical), dipicolinic acid (>98%, Sigma-Aldrich), sodium hydroxide (0.25 N, Ricca Chemical), ceric sulfate (0.25 N, GFS Chemical), potassium hydrogen phthalate (>99.9%, NIST), arsenic trioxide (>99.9%, Alfa Aesar), and osmium trioxide (>99, Alfa Aesar) were all gathered from production or purchased and used as received. No other purification was deemed necessary since impurities in the chemicals were negligible per the certificate of analysis for the purposes of this experiment.

2.2 Synthesis and Control of Peracetic Acid Samples

Samples were prepared in the lab following a batch method of mixing the components in the appropriate ratios leading to specific equilibrium concentrations of peracetic acid and hydrogen peroxide. These samples were carefully made to prevent contamination from metals or any other materials that may lead to the decomposition of the formulation. Sample containers were made of glass and containers were passivated before use. The passivation technique used in this experiment was to soak the glassware in 10% nitric acid overnight then rinse and dry. Typically, the samples were made in triplicate with a volume of 50 mL. Depending on the designation, samples were either kept inside a

chemical cabinet for room temperature assay tracking or inside incubators for high temperature tracking. The incubators were held at temperatures ranging from 35-60°C and the incubators were periodically checked to verify the temperature. The samples were assayed periodically and the length of time that they were tracked was dependent on the temperature. Room temperature samples were tested for up to a year and the higher temperature samples were tracked up to 6 weeks.

2.3 Auto-titrator Instrument

Sample analysis was performed using a Metrohm autotitrator with Tiamo software version 1.2.1. The peracetic acid titration is done by 3-point pH detection equipped with an 854 iConnect probe (model 6.0278.300). The titration uses equivalence points, which are similar to an inflection point in an acid-base titration. This point is where the reagent and the analyte are in equal concentrations. The volume of reagent that was required to reach this point is used in the final calculation to determine the concentration of the equilibrium mixture of acetic acid and peracetic acid. These analytes in solution can be distinguished from one another because of the difference in pKa values. The pKa values for acetic acid and peracetic acid are 4.76 and 8.20, respectively. Figure 13 shows a typical determination curve for the titration of PAA. The midpoint between endpoint 1 and 2 is the pKa of acetic acid and the midpoint of 2 and 3 is approximately the pKa of peracetic acid. The initial end point is from stabilizer that is found in the sample. The titration only takes a few minutes from

start to finish so a shift in the equilibrium between the various components in not a concern.

The auto-titrator then needs to be converted to assay the hydrogen peroxide concentration. This method uses a potentiometric endpoint using an 854 iConnect probe (model 6.0451.300). The hydrogen peroxide is titrated with ceric sulfate until an endpoint is detected as shown in Figure 14.

Due to the nature of a PAA equilibrium mixture, no standard exists to calibrate, standardize or check the performance of the instrument.
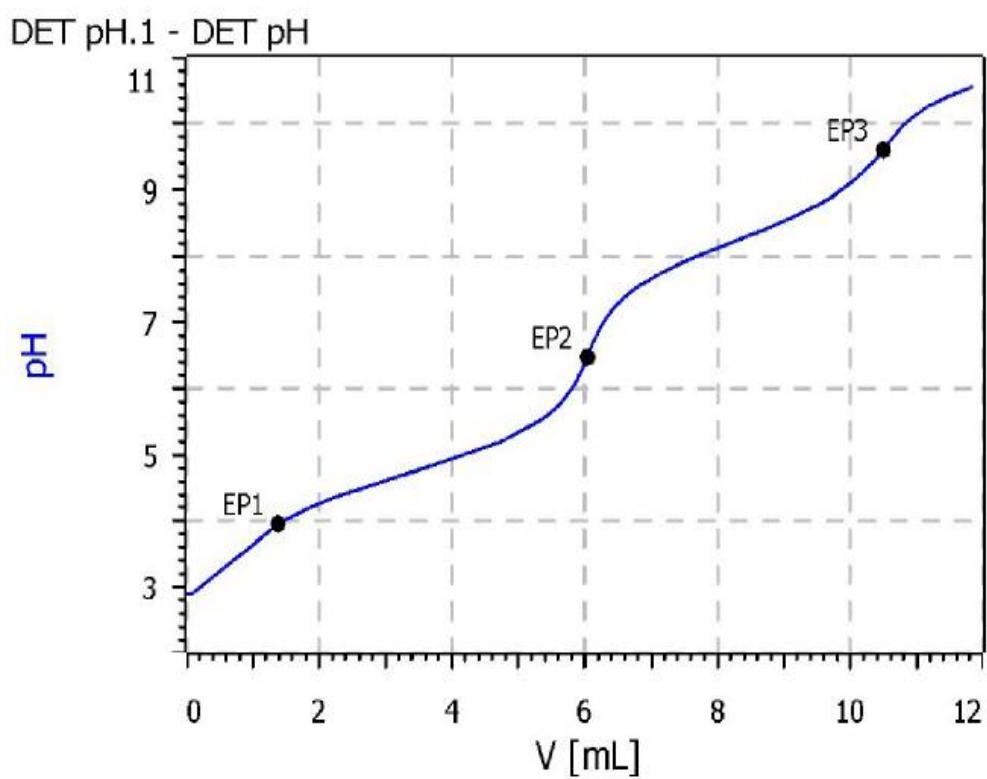
Figure 13: Example of a PAA analysis curve of a sample that consists of equivalent amounts of peracetic acid and acetic acid in this case. Sample titrations only proceed for a few minutes which does not cause significant changes to the equilibrium. This allows for an accurate result for the PAA and acetic acid concentrations.
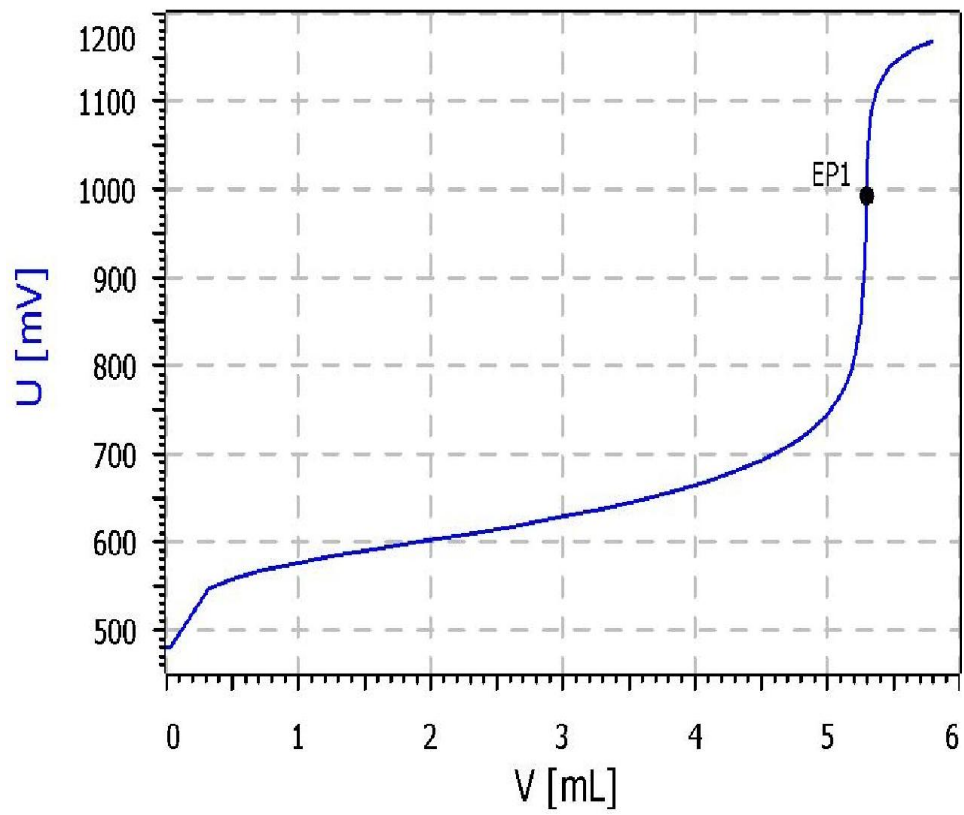
Figure 14: Example of a potentiometric titration of hydrogen peroxide with ceric sulfate.

2.4 Titrant Standardization

The titrants used to titrate the PAA and hydrogen peroxide are checked with established methods primarily found in the American Society for Testing and Materials (ASTM International) [38]. Typical manual methods use an end point indicator. Since the standardization is done by autotitrator, there is no need for an indicator. The absence of an indicator does not affect results, as it is used only for visual representation of the end point when testing manually.

Sodium hydroxide is checked using potassium hydrogen phthalate traced to the NIST standard reference material. The standardization is done in a series of 5 samples with approximately 1.0 g of the phthalate standard. This standard is diluted with 100 mL of high purity water and tested on the autotitrator. The average of the 5 samples is used as the normality of the sodium hydroxide and the instrumentation is adjusted accordingly.

The ceric sulfate standardization is a little more complex due to the hazardous nature of the compounds used for the test. The standardization is also done in a series of 5 samples using about 0.2 g of arsenic trioxide. Arsenic trioxide is then dissolved in 20 mL of 10% sodium hydroxide. When solution is complete, 50 mL of DI water is added along with 10 mL of 25% sulfuric acid and 3 drops of osmium tetroxide. When the titrations are completed, the average of the 5 samples is used for the normality value.

2.5 Differential Scanning Calorimeter (DSC)

The DSC 1 from Mettler-Toledo is calibrated by a pure metal that has a known melting point and enthalpy. This instrument uses indium as the calibration metal which has a melting point at 156.60°C with an allowable value of 156.30-156.90°C. The normalized enthalpy of the melt should be between 27.85 $^J/_g$ and 29.05 $^J/_g$. The instrument should be checked with the calibration metal often due to the volatile nature of the chemicals used. If a value falls outside the melting point or enthalpy range, the instrument needs to be calibrated.

The instrument adjustment is rather simple and can be done by conducting at least 5 indium checks. A small pill of indium is placed into a 40 µL aluminum crucible and pressed to the bottom for good contact. The crucible is then hermetically sealed to be placed into the DSC furnace. The DSC indium check method is used to check the calibration and to adjust the instrument. This method tests the temperature range from 120°C to 180°C at a scanning rate of 10°C/min. The melting temperature and the normalized enthalpy is averaged and input into a calibration screen. Once the values are adjusted, another check should be done. The instrument should now be within specifications. An example is an indium trace is shown in Figure 15.

Once the temperature and enthalpy was calibrated, the enthalpy values of PAA decomposition were tested using temperature rates of 3, 5 and 10°C over a temperature range of 30-150°C. The rates were varied because scanning rate can change the maximum temperature of the exotherm and to see how the

formulation behaved under various heating rates. This maximum temperature

can be used as an alternate way to determine the activation energy.
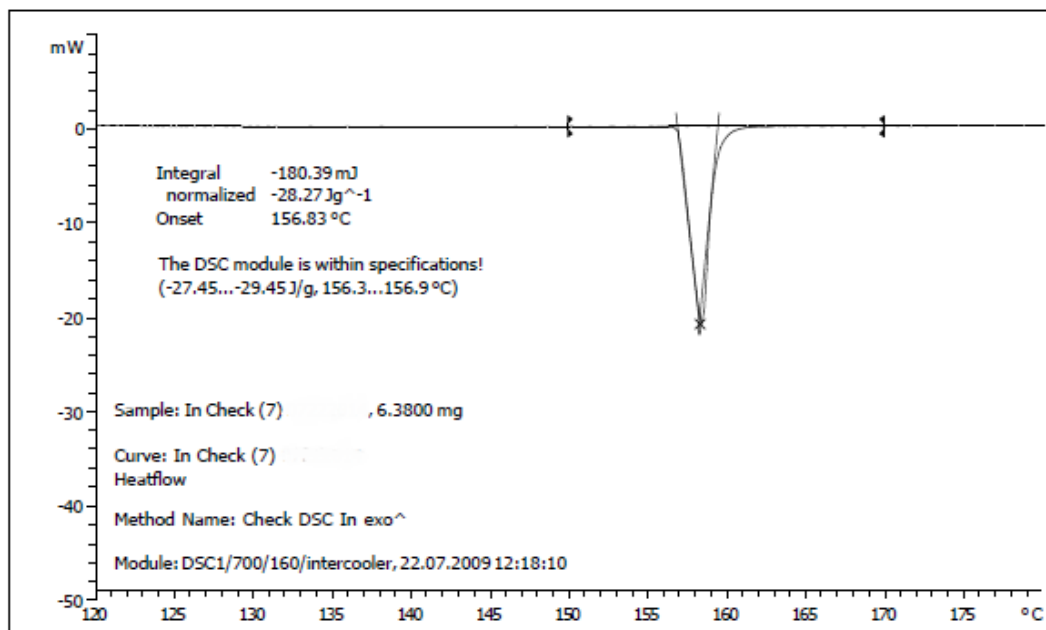
Figure 15: Typical DSC trace for indium calibration. This is tested with a pre-programmed method that is provided into the instrument.

Chapter 3: Results

3.1 Determination of Decomposition Kinetics for the Various Formulations

The starting point to determine parameters like activation energy and pre-exponential factor is to determine the decomposition kinetics of a formulation. Several formulations were tracked over time and the degradation of the PAA and hydrogen peroxide are plotted. A typical chart that is created is shown in Figures 16 and 17. The assays of the samples are tested periodically over an extended period of time. The time they are tracked is usually dependent on the temperature that the samples are being stored in.

Since the Arrhenius equation is dependent on temperature, one must use at least 3 different temperatures to extrapolate the activation energy and pre-exponential factor. It is important to get as many data points as possible to get a proper correlation and confirm the plot is linear. Once enough data is collected, the formulation is converted to total active oxygen for the PAA and hydrogen peroxide by calculation. This data is used to determine the decomposition rates as shown in Figure 18 by plotting the natural log of the normalized active oxygen concentration versus time. Table 2 shows all the rates that were determined at various temperatures with all the formulations.
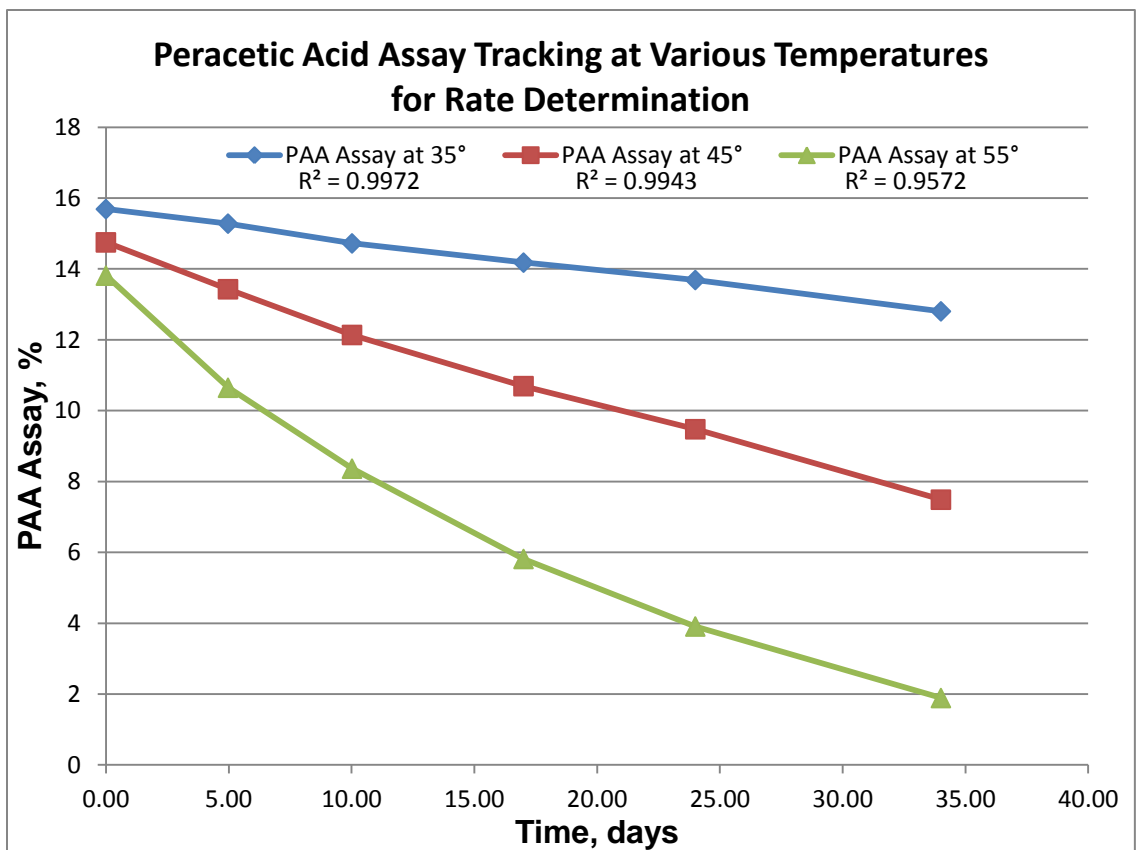
Figure 16: Example of the reduction in PAA assay over time at various temperatures. This degradation shows first order kinetics.
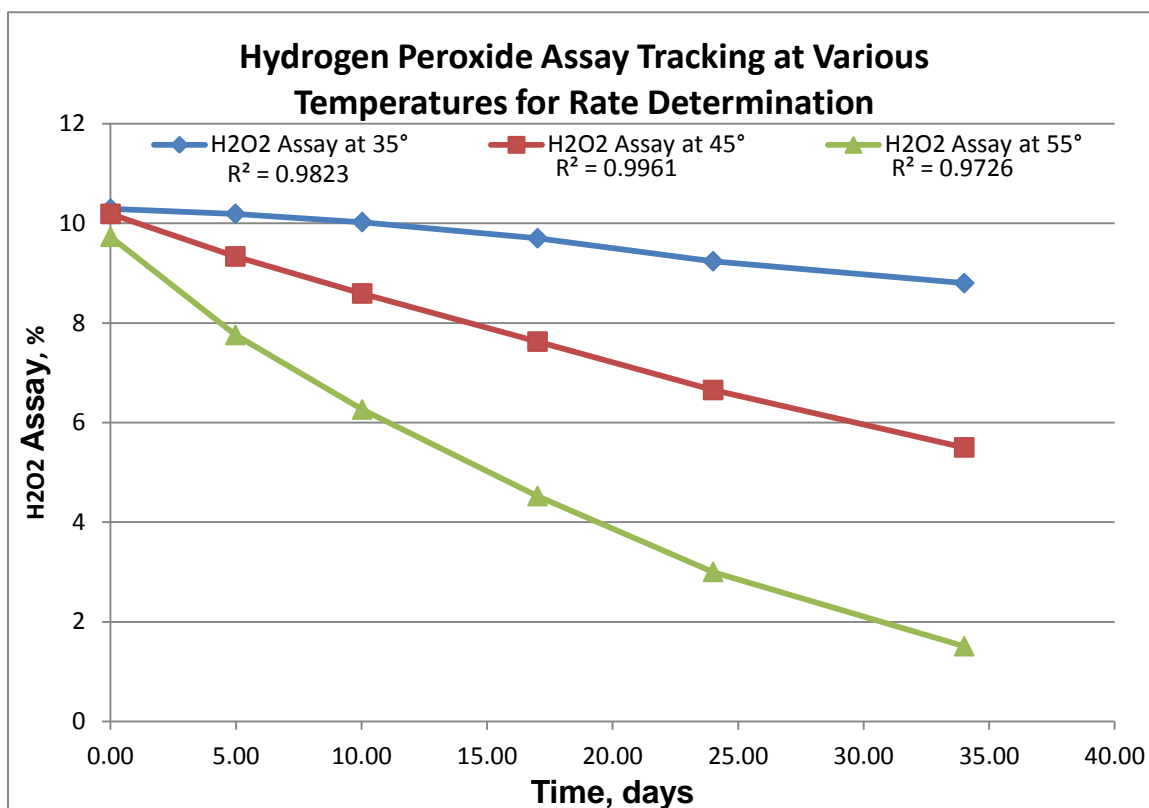
Figure 17: Example of the reduction of hydrogen peroxide over time at various temperatures. Again, decomposition appears to be first-order.
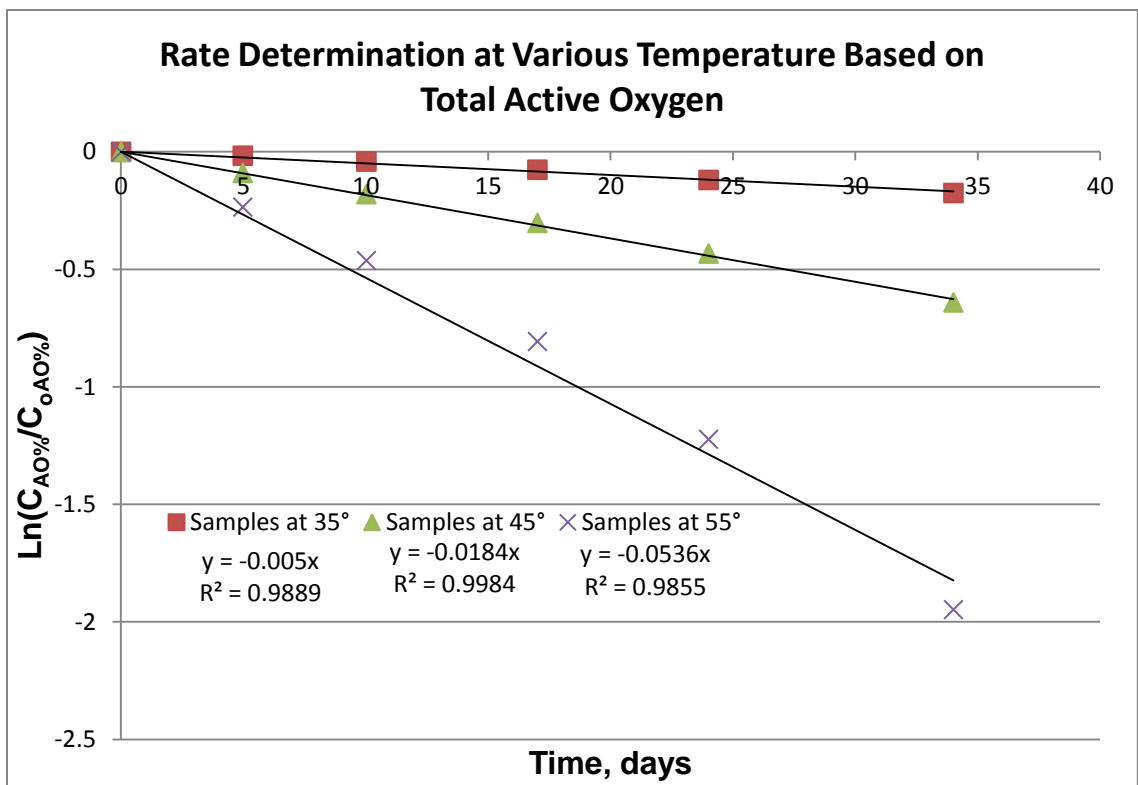
Figure 18: Chart used to determine the decomposition rate of the total active oxygen at various temperatures. The slope translates to the negative rate of decomposition.

Table 2: Average rate for each formulation at various temperatures with respect to active oxygen loss. Samples were tested in triplicate so that the standard deviations could be calculated. Formulation 4A and 5A was only tested as a single sample at room temperature. These values were later used to determine the kinetic parameters.

Formulation	Room Temperature Avg.	Std. Dev.	35°C Avg.	Std. Dev.	45°C Avg.	Std. Dev.	50°C Avg.	Std. Dev.	55°C Avg.	Std. Dev.	60°C Avg.	Std. Dev.
1A	-8.0E-05	1.8E-05			-4.7E-04	2.0E-04	-1.1E-03	4.5E-05				
1B	-2.2E-05	1.5E-05			-7.5E-04	1.3E-04	-1.3E-03	1.0E-04				
1C	-1.1E-04	3.2E-05			-1.1E-03	1.2E-04	-1.3E-03	2.3E-04				
1D	-2.5E-05	1.7E-05			-1.2E-03	1.7E-04	-1.4E-03	1.1E-04				
1E	-8.0E-05	5.7E-06	-2.7E-04	2.4E-05					-1.4E-03	2.3E-04		
1F	-1.3E-04	1.5E-06	-3.6E-04	6.6E-05					-2.1E-03	1.9E-04		
2A			-7.3E-04	6.4E-05	-2.2E-03	5.2E-04			-4.9E-03	1.4E-03		
3A	-1.5E-04	1.5E-05	-5.3E-04	2.3E-05					-3.7E-03	1.3E-03		
3B	-2.0E-04	2.3E-05	-7.2E-04	2.7E-05					-3.5E-03	2.8E-04		
3C			-1.4E-03	9.4E-05	-3.7E-03	3.3E-04			-2.3E-02	2.1E-02		
4A	-2.0E-03				-6.2E-03	1.1E-03	-3.3E-02	2.0E-03			-5.3E-02	1.8E-03
5A	-6.9E-04				-5.6E-03	1.6E-03	-1.0E-02	2.2E-04			-1.5E-02	7.0E-04

3.2 Determination of Activation Energy and Pre-exponential factor

Once the rates were determined and found to be simple first-order, plots were derived using the natural log of the decomposition rate versus the reciprocal temperature. The slope of the curve provides the activation energy divided by the gas constant while the y-intercept is the natural log of the pre-exponential factor. A typical plot is shown in Figure 19. Table 3 shows all the calculated activation energies and pre-exponential factors that were found using this method.
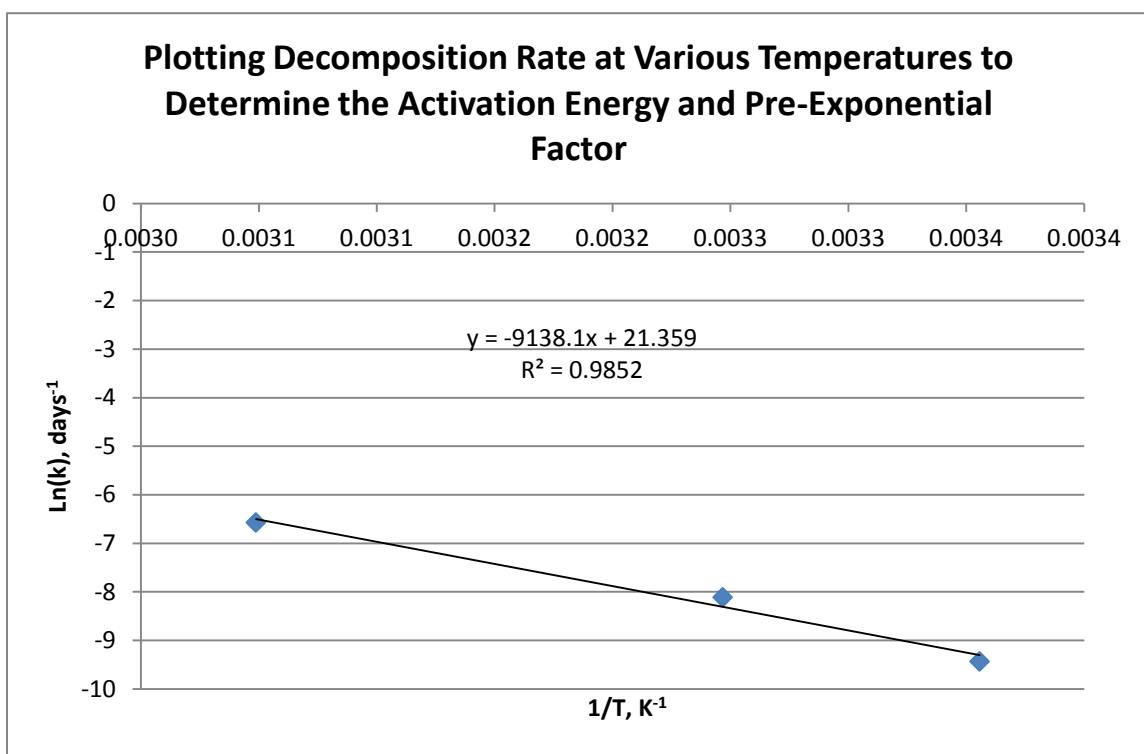
Figure 19: Plot of decomposition rates over various temperatures to determine the activation energy and pre-exponential factor

Table 3: Calculated values for activation energy and pre-exponential factors for the various formulations based off of the Arrhenius equation.

Formulation	$E_a,$ $^{kJ}/_{mol}$	A, days^{-1}
1A	66.6	4.61E+07
1B	108	3.46E+14
1C	80.8	1.67E+10
1D	122	7.31E+16
1E	76.0	1.89E+09
1F	80.9	1.73E+10
2A	80.1	2.77E+10
3A	94.8	4.45E+12
3B	84.4	1.23E+11
3C	105	6.57E+14
4A	81.2	3.89E+11
5A	75.3	1.09E+10

3.3 Enthalpy of Decomposition of PAA Solutions

Several different PAA formulations were tested on the DSC to determine the energy given off by the decomposition of PAA. Table 4 shows the different enthalpy values that were determined.   Small variations in the experiments were used to capture the full range of the enthalpy along with changes in the heating rates to monitor any changes in the maximum temperature that was reached. Table 5 shows a comparison of formulations between an outside lab and the testing done in this experiment.

When the decomposition enthalpy of the formulations were plotted versus the active oxygen content there is a somewhat linear correlation. This presents the possibility that the decomposition energy could be extrapolated based on the active oxygen content of the formulation. The plot in Figure 20 shows this correlation.

Table 4: Enthalpy values of various PAA formulations along with some simple statistics. These values show some dependence on the active oxygen of the formulation.

Sample	Rep.	AO, %	$\Delta H, {}^J/_g$	$({}^J/_g)/AO,\%$	Avg. ΔH	Std. Dev. ΔH	%RSD
15564-8	1	14.45	1170	81.0			
15564-8	2	14.45	971	67.2			
15564-8	3	14.45	1214	84.0	1160	105.0	9.05
15564-8	4	14.32	1200	83.8			
15564-8	5	14.32	1220	85.2			
Batch 2	1	7.25	781	108			
Batch 2	2	7.25	763	105	755	40.7	5.39
Batch 2	3	7.25	695	96			
Batch 2	4	7.25	780	108			
15567-1	1	14.22	1510	106.2			
15567-1	2	14.22	1240	87.2			
15567-1	3	14.22	1350	94.9	1340	102.0	7.61
15567-1	4	14.22	1290	90.7			
15567-1	5	14.22	1330	93.5			
2004270	1	8.20	785	95.7			
2004270	2	8.20	656	80.0			
2004270	3	8.20	661	80.6	711	53.9	7.58
2004270	4	8.20	717	87.4			
2004270	5	8.20	735	89.6			
2004940	1	10.30	783	76.0			
2004940	2	10.30	797	77.4	798	14.3	1.79
2004940	3	10.30	817	79.3			
2004940	4	10.30	793	77.0			
15564-4	1	14.53	1380	95.0			
15564-4	2	14.53	1300	89.5	1350	43.6	3.23
15564-4	3	14.53	1370	94.3			
2002955A	1	8.34	673	80.7			
2002955A	2	8.34	651	78.1	658	13.3	2.02
2002955A	3	8.34	649	77.8			
2004458	1	11.47	1030	89.8			
2004458	2	11.47	1020	88.9	1030	5.8	0.56
2004458	3	11.47	1030	89.8			

Table 5: Comparison of enthalpy values that were determined within this experiment and an outside lab for verification.

	Experimental Results			External Testing		
	ΔH, J/g	σ	%RSD	ΔH, J/g	σ	%RSD
Formulation 1	1240	111	8.9	1180	208	17.7
Formulation 2	610	48.7	8.0	944	NA	NA
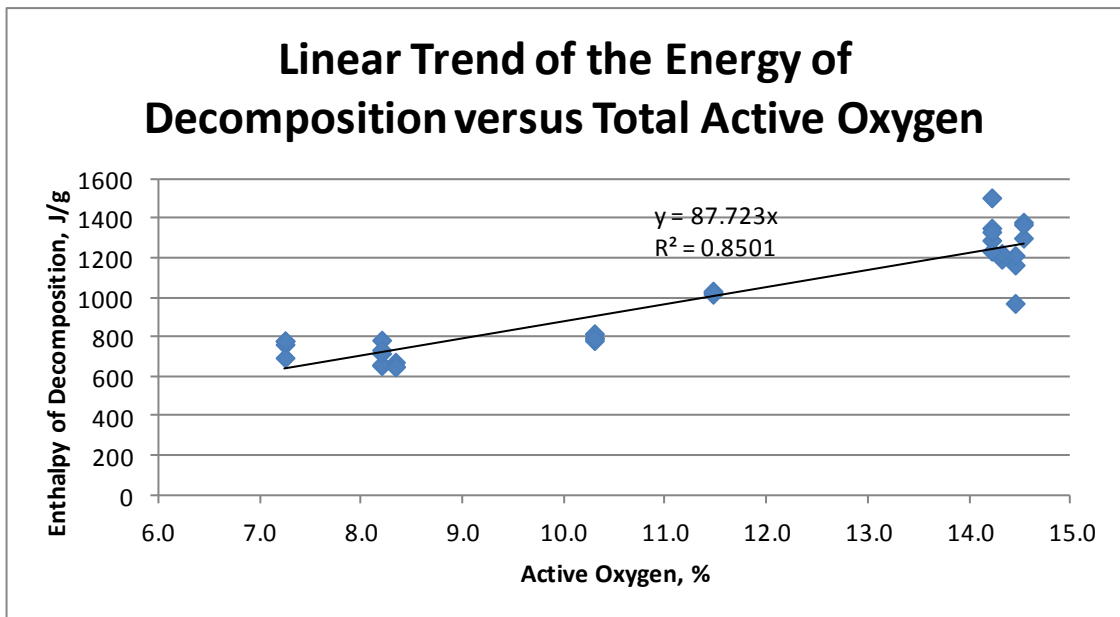
Figure 20: Analysis of the energy of decomposition versus the total active oxygen of various formulations. There is a linear trend with some unexplained variation.

3.4 Self Accelerating Decomposition Temperatures (SADT)

Using all the previous calculations, the SADT can be calculated for various formulations in several different packages and sizes. Table 6 shows the various SADT values that were calculated by this method along with comparison values from outside labs in Table 7. Another calculation was done on the SADT values to see how various parameters affect the final value. This was done by varying the activation energy, pre-exponential factor and exothermicity by +/- 10%. Results are shown in Table 8.

Table 6: SADT Values for Formulations Tested in Various Packages.

Formulation	225 kg Drum, °C	1500 kg Tote, °C	25000 kg Bulk, °C
1A	94.9	82.3	80.2
1B	66.5	60.1	59.0
1C	74.3	65.2	63.6
1D	61.8	56.3	55.3
1E	82.5	72.3	70.6
1F	74.2	65.1	63.6
2A	73.9	64.7	63.1
3A	71.1	63.5	62.2
3B	71.7	63.1	61.6
3C	55.2	49.0	47.9
4A	42.2	34.8	33.5
5A	59.6	50.6	49.1

Table 7: Comparison of SADT values that were calculated using the method described in this paper along with values that were calculated by outside labs using UN/DOT approved methods.

Formulation	Experimental		Lab #1		Lab #2					
					Replicate 1		Replicate 2		Replicate 3	
	55 Gal., °C	Tote, °C	55 Gal., °C	Tote, °C	55 Gal., °C	Tote, °C	55 Gal., °C	Tote, °C	55 Gal., °C	Tote, °C
1B	66.5	60.1	46.0	39.0	64.9	60.2	50.1	45.4	82.2	79.6
1C	74.3	65.2	46.0	39.0	64.9	59.8				
1D	61.8	56.3			>75	>75	51.4	44.0		
1E	82.5	72.3	56.6	50.9	80.0	75.0				
1F	74.2	65.1	52.0	47.0	60.0	55.5				
2A	73.9	64.7	60.9	54.6	80.0	75.0				

Table 8: Variation of calculated parameters +/- 10% to show the effects of minor errors in determining these values. These calculations are based on a 1500 kg SADT value. Temperatures presented are in °C.

Formulation	1500 kg	ΔEa, +10%	ΔEa, -10%	ΔA, +10%	ΔA, -10%	ΔH, +10%	ΔH, -10%
1A	82.3	119.7	45.1	80.7	84.2	80.7	84.2
2A	64.7	99.8	29.7	63.5	66.1	63.5	66.0
3A	63.5	98.3	28.8	62.5	64.6	62.5	64.6

Chapter 4: Discussion

4.1 Decomposition Kinetics to Determine Activation Energy and Pre-exponential Factor

The kinetics parameters of the reaction are fairly straight-forward and easy to calculate due to the first-order decomposition observed. Referring back to Table 2, we show the various decomposition rates that were calculated from the data. The rates trended as expected with the fastest rate of decomposition at the highest temperature. None of the data deviated from first-order kinetics although there were some data points that showed some sizeable variation. This is expected since titrations do not have a significantly high degree of accuracy regardless of automation. Weighing errors, errors in titrant standardization and misinterpretation of endpoints for the concentration calculations can contribute to variation. This was resolved by testing the samples in triplicate and averaging the values to reduce the total variation.

The rates for each formulation were on the same relative scale at each temperature tested. A commonly stated rule of thumb is that the rate doubles for every 10°C temperature increase. In this case, this rule is a reasonable estimate. The decomposition rates varied slightly for each different type of formulation. It appears that the higher the hydrogen peroxide concentration, the slower the decomposition was. This falls in line with kinetics because hydrogen peroxide is much more stable than peracetic acid. Since PAA decomposes into acetic acid and water, these product turn to reactants that reform PAA. This helps maintain the chemical equilibrium of the formulation.

Referring back to Table 3, the data shows the activation energy and the pre-exponential factor were fairly consistent within the different formulations that were tested, even with the large variation in the decomposition rates. The determined values compared well to the few values found in literature. The values also coincide with values obtained from samples that were verified at third party laboratories. Literature values of 66.15 $^{kJ}/_{mol}$ and 70.20 $^{kJ}/_{mol}$ were found [38, 39] and somewhat compare to the experimental values determined here. The activation energy value also makes sense when comparing to other peroxygen compounds from Table 1. Since PAA is less stable, it makes sense that the energy required to start decomposition will be lower than the other peroxygen compounds.

4.2 Enthalpy of Decomposition Determination

It was difficult to find a good method that would be able to accurately determine the values with good reproducibility. The values obtained in this experiment versus some tests that were performed at outside labs compare well, with the internal tests being more accurate. Two of the formulations were sent for testing and the results are shown in the Table 5. The tests that were run during this experiment showed lower percent replicate standard deviation (% RSD) value, which shows better reproducibility. Increased experience led to improvements in experimental data collection and analysis.

Using the values that were found in Tables 4, an effort was made to determine a linear equation that could be used to calculate the enthalpy values. First, a simple linear regression was executed comparing the active oxygen in the formulation versus the energy from the decomposition of the formulation. Figure 19 shows this plot. This

is a good correlation but there is still some unexplained variation. Another step was to use a multiple regression using all the components from the formulation to see if there is some contribution from the acetic acid and the water. The multiple regression that included the moles of peracetic acid, hydrogen peroxide, acetic acid and water had a high correlation with an R^2 of 0.992. However, the p-value that was associated with the acetic acid value was over 0.05 and the water value was highly correlated with other variables and was removed. The equation was as follows:

$$H, kJ = 93.5 * (PAA, moles) + 156.0 * (H_2O_2, moles) + 0.63$$
$$* (Acetic\ Acid, moles) \qquad\qquad (32)$$

The next regression removed the acetic acid and water value to see how the equation fit with the molar values of PAA and hydrogen peroxide separated. This time the R^2 was also 0.992 but the p-values for each were lower than 0.05. The linear equation is:

$$H, kJ = 94.41 * (PAA, moles) + 155.61 * (H_2O_2\ moles) \qquad\qquad (33)$$

The equation only has minor changes to the coefficients for PAA and hydrogen peroxide. It also makes sense because the majority of the energy of the decomposition will come from the PAA and hydrogen peroxide with some energy being consumed by the vaporization of water and acetic acid.

The coefficients in Eq. (33) should correspond to known values of the enthalpy of decomposition. For hydrogen peroxide, a value found for the heat of decomposition is 187.8 $^{kJ}/_{mole}$. This value is high compared to the coefficient in the above equation but the enthalpy values found by the DSC may not be as large in magnitude as it should be. Since the crucible is sealed, this will raise the pressure, in turn, raising the boiling points

of the compounds in the formulation. This will only help so much so the extent of the

energy release of the formulation may be varied due to the amount of volatiles in the

vapor space. It is assumed that the coefficient for PAA is also lower than other methods

but literature data for PAA has not been found.

Some methods have been found in literature that use various parameters

determined from the DSC to also establish the values of activation energy and pre-

exponential factor. Many of these methods only require the heating rate of the sample,

maximum temperature of the exotherm and a fractional rate of reaction. An example of

this is a method developed by Homer Kissinger. This method plots the heating rate of

the sample versus the maximum temperature of the exotherm [41]. This method is not

valid for this type of work because these formulations sometimes decompose with two

different peaks in the exotherm depending on the concentrations of PAA and hydrogen

peroxide. Figure 21 shows an example of the issue. It is possible to determine the

maximum value for each but, when it comes to determining the formulations kinetic

parameters, it is better to simplify the calculation by using the energy from the full

decomposition. At a minimum, utilizing the full decomposition energy and using it as a

worst-case scenario can be performed.
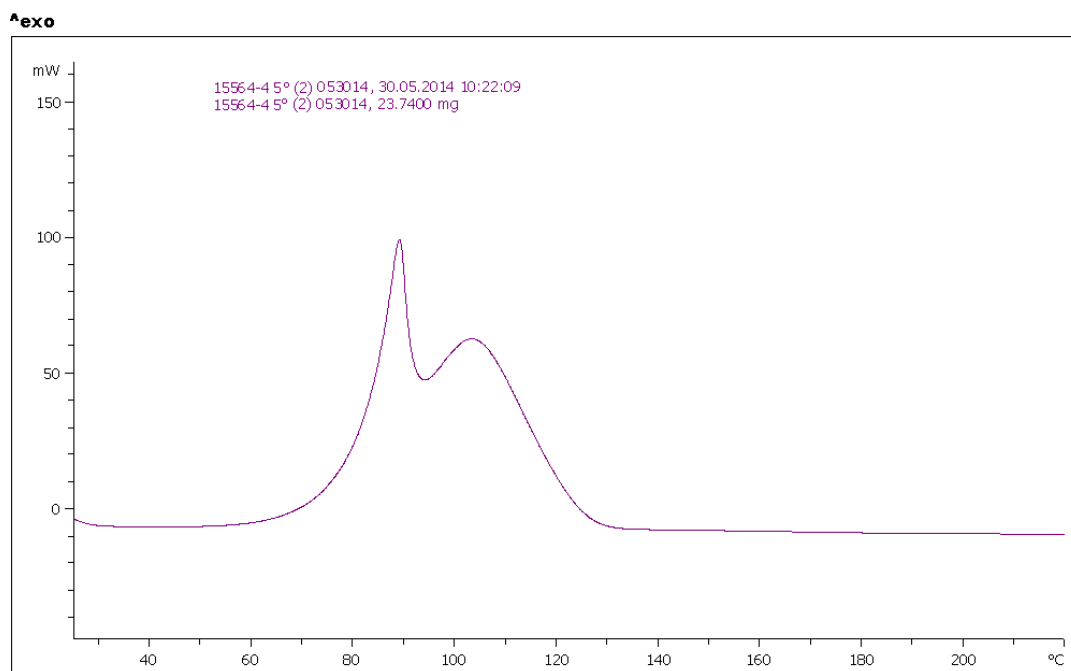
Figure 21: Trace for the decomposition of a formulation with two peaks. We theorize that the PAA decomposes first giving the first peak followed by hydrogen peroxide at a higher temperature.

4.3 SADT Values for Various Formulations

The SADT values in Table 6 show that there is a large variation even within the same type of formulation. It is worthwhile to see that small changes within the formulation can be resolved in order to make a final determination to move forward with more development work. The values also tend to be more conservative since the surface area used is based on the surface of a sphere for packages or container sizes in practice. The image shown in Figure 22 shows that the surface to volume ratio is the lowest when using the surface area of a sphere. This helps to keep the values that are calculated here conservative versus using the actual shape of a package.
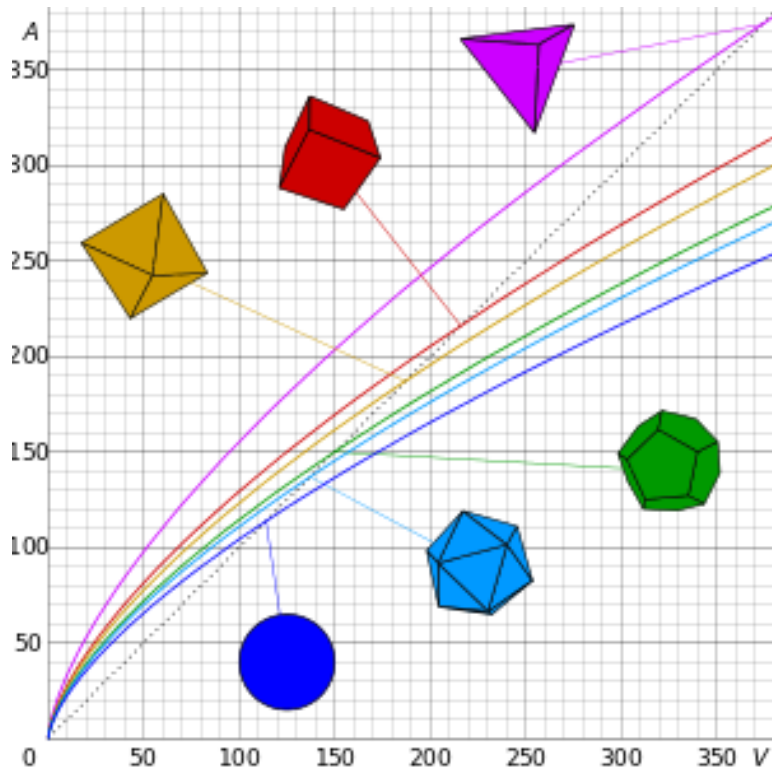
Figure 22: Surface to volume ratios of various shapes. The spherical shape shows a conservative view of the surface to volume ratio of all the geometric shapes [42].

It is also important to note the changes that relate with changes in the various

parameters. The activation energy is the most critical since a relatively small change of

10% can have a significant impact on the final value. Looking at Eq. (12), it makes

sense since this parameter is tied to the exponential. When the pre-exponential factor

was varied, the inverse change in values compared to what was seen with the activation

energy seems logical since this value is also viewed as a collision factor. If the number

of collisions is increased then this would lower the temperature required to initiate the

decomposition.

It is difficult to state whether this method completely agrees with outside labs

since outside lab results do not compare well to each other. The limited data available

in literature also makes it difficult to validate this method. Each lab conducted the test in

a different manner. Lab #1 conducted the test with a TAM microwatt calorimeter while

lab #2 tested the samples using an adiabatic testing chamber. Chapter 1 has a

description of the other methods. It was instructed to each lab to passivate all surfaces

that will come into contact with the formulation to prevent any outside contamination that

will bias the results. With each lab conducting the testing in different ways, there is an

expectation of some differences in the final calculated value. However, there is also the

expectation that these validated tests will predict the SADT value within 5°C of each

other.

The values that were acquired from outside testing shown in Table 7 have quite a

bit of variability between labs with each sample. There also appears to be quite a bit of

variation within the same formulation. The values for the SADT that were calculated in

this study are similar to outside labs and found with similar variation within the same

formulation. Formulation 1D displays a rare exception when a lab was unable to detect an exotherm over the course of the test. The value shown is counter to what one would expect with a peroxygen compound and does not compare to any value that was found during this study or at the other lab that conducted the test. This could have been due to a leak or contaminant in the system.

Chapter 5: Conclusion

The kinetic data that was calculated by the means described in this paper using simple kinetic equations along with simple concentration monitoring over time were reasonable with some differences present between the formulations. There are some concerns about the variation in some of the rate constants but this is most likely due to titration error. It would be beneficial for future work to increase the amount of replicates with the formulations to provide the opportunity to do some better statistical analysis. This could either help to determine if the cause of the high standard deviations is truly from titration error or possibly from the complex equilibrium of the formulations.

Once the Arrhenius parameters were calculated, the values looked fairly consistent between the formulations. There were a couple formulations that stood out with significantly higher or lower activation energies. However, there was an overall trend of the system having lower activation energy compared to other organic peroxides. These values are justified since the potential for violent decompositions is inversely related to the peroxygens molecular weight [1].

The enthalpy data seemed consistent and reproducible when the data was compared to outside labs. The data fit a multi-linear equation when the different components were used rather than fitting only the active oxygen versus heat of decomposition. This makes sense because the energy given off by each compound should be different rather than assuming that it is the same from each active component. In the case of the coefficients for the multiple regressions, some additional work should be done to determine the equilibrium shift when the temperature is

increased in the system. This could help increase the coefficient on hydrogen peroxide to referenced bond enthalpies. This may indirectly help to determine a value for peracetic acid in the liquid phase.

The self-accelerating decomposition temperatures appeared to be consistent with the method described in this work. Data generated within this study appeared to be more consistent than the data generated by outside labs. This indicates that this method is a potentially reliable way to screen new formulations for SADT values. Additional research would have to be performed in order to conclude that method described in this work is consistently more reliable than previously used methods performed in outside labs.

A viable next step would be to try to use a different type of Arrhenius equation that is derived from the Transition State Theory. Eq. (34) relates the translational, rotational and vibrational contributions of the molecules during the reaction. The main Arrhenius equation is derived from the collision theory that assumes that molecules are hard spheres rather than complex geometrical shapes. Due to this difference, there should be some differences in the calculated kinetics between the two equations. This equation also takes into account the concentrations of the activated complex along with the concentrations of the reactants that forms the activated complex [22].

$$k = \kappa \frac{k_b T}{h_o} \frac{Q^{\neq *}}{Q_x Q_{yz}} \exp\left(\frac{-E_o}{RT}\right) \tag{34}$$

Another idea would be to see how this applies to formulations with significant changes to the equilibrium. Typically, these cases only applied small additions of stabilizers or catalysts on the order of less than 1% of the total formulation. It would be

interesting to see if this method would apply to significant increases of these additives

on the order of multiple percent. It would be assumed that this method would still apply

as long as the decomposition kinetics continues to trend as first-order.

References

[1] Clark, D. E., *Chem. Health. Saf*, 8, 12-22, 2001.

[2] Varjavandi, J.; Mageli, O. L. *J. Chem. Ed*. 48, 451-456, 1971.

[3] Nagel, M., *J. Chem. Ed.* 61, 250-251, 1984.

[4] Bretherick, L., *Improving Safety in the Chemical Laboratory: A Practical Guide*. New York. John Wiley & Sons. 1987.

[5] Leveneur, S., Catalytic Synthesis and Decomposition of Peroxycarboxylic Acids. Dissertation, University of Abo. France. (NNT : 2009ISAM0005).

[6] Dell'Erba, A.; Falsanisi, D.; Liberti, L.; Notarnicola, M.; Santoro, D., *Desalination* 215, 177-186, 2007.

[7] Bauermeister, L. J.; Bowers, J. W. J.; Townsend, J. C.; McKee, S. R. *Poult. Sci.* 87, 2390-2398, 2008.

[8] Kralovic, R.C.; Badertscher, D. C. Anti-Microbial Composition. Steris Corp., assignee. Patent 5,077,008. 31 Dec. 1991.

[9] Nakayama, M.; Hosoya, K.; Tomiyama, D.; Tsugukuni, T.; Matsuzawa, T.; Imanishi, Y.; Yaguchi, T. *J. Food Protect.* 76, 999-1005, 2013.

[10] Abdel-Halim, E. S.; Al-Deyab, S. *Carbohyd. Polym.* 86, 988-994, 2011.

[11] Cox, D. P.; Zhang, Y.; Zhang, W.; and James, K. E., Process for Preparing Oxycodone Having Reduced Levels of 14-hydroxycodeinone. Noramco, Inc., assignee. Patent 7,906,647. 15 Mar. 2011.

[12] Yuan, Z,; Ni, Y.; Van Heiningen, A. *Can. J. Chem. Eng*. 75, 37-41, 1997.

[13] Zhao, X.; Cheng, K.; Hao, J.; Liu, D. *J. Mol. Catal. A – Chemical.* 271, 246-252, 2007.

[14] Kadla, J.; Chang, H. The Reactions of Peroxides with Lignin and Lignin Model Compounds. In *Oxidative Delignification Chemistry;* Argyropoulos, D., ACS Symposium Series; American Chemical Society: Washington, DC, 2001; 108-129.

[15] Brown, D.; Abbot, J. *J. Wood Chem. Tech.* 15, 85-111, 1995.

[16] Barbusinski, K., *Ecol. Chem. Eng.* 16, 347-358, 2009.

[17] Singh, R., *Tappi.* 49, 281-286, 1966.

[18] Hart, R., *Tappi*. 64, 43-44, 1981.

[19] Colodette, J.; Fairbank, M.; Whiting, P. *J. Pulp Pap. Sci.* 53, 16-18, 1990.

[20] Wu, L.; Chen, K.; Cheng, S.; Lee, B.; Shu, C. *J. Therm. Anal. Calorim.* 93, 115-120, 2008.

[21] Zukas, J. A., *Explosive Effects and Applications*. New York. Springer Science and Business Media. 1998.

[22] Kotoyori, T. *Critical Temperatures for the Thermal Explosion of Chemicals*. Amsterdam. Elsevier B.V. 2005

[23] *Transport of Dangerous Goods: Extracts from Recommendations Prepared by the United Nations Committee of Experts on the Transport of Dangerous Goods, As Amended by the United Nations Committee of Experts for Further Work on the Transport of Dangerous Goods*. New York: United Nations, 2005.

[24] Petrucci, R. H.; Harwood, W. S.; Herring, F. G., *General Chemistry*. New Jersey. Prentice Hall. 2002.

[25] Wright, M. R., *An Introduction to Chemical Kinetics*. New Jersey. John Wiley & Sons, Ltd. 2004.

[26] Wang, Q.; Rogers, W. J.; Mannan, M. S., *J. Therm. Anal. Calorim.* 98, 225-233, 2009.

[27] Liu, S.; Lin, C.; Shu, C. *J. Therm. Anal. Calorim.* 106, 165-172, 2011.

[28] Duh, Y.; Yo, J.; Lee, W.; Kao, C.; Hsu, J. *J. Therm. Anal. Calorim.* 118, 339-347, 2014.

[29] Wu, S.; Chi, J.; Huang, C.; Lin, N.; Peng, J.; Shu, C. *J. Therm. Anal. Calorim.* 102, 563-568, 2010.

[30] Wu, S.; Chou, H.; Pan, R.; Huang, Y.; Horng, J.; Chi, J.; Shu, C. *J. Therm. Anal. Calorim.* 109,355-364, 2012.

[31] You, M.; Liu, M.; Wu, S.; Chi, J.; Shu, C. *J. Therm. Anal. Calorim.* 96, 777-782, 2009.

[32] Goldberger, M.; Watson, K. *Collision Theory*. New York. Dover Publications. 1964.

[33] Wright, M. R. *An Introduction to Chemical Kinetics*. New Jersey. John Wiley & Sons. 2004.

[34] Larsen, D. (2013, October 2). Transition State Theory. Retrieved October 27, 2015, from http://chemwiki.ucdavis.edu/Physical_Chemistry/Kinetics/Modeling_Reaction_Kinetics/Transition_State_Theory/Transition_State_Theory

[35] Musuc, A. M.; Razus, D.; Oancea, D. *J. Therm. Anal. Calorim.* 90, 807-812, 2007.

[36] Mettler-Toledo AG. (2011). *Differential Scanning Calorimetry for all Requirements* [Brochure]. Schwerzenbach, Switzerland.

[37] ASTM Standard E2070, 2008, "Standard Test Method for Kinetic Parameters by Differential Scanning Calorimetry Using Isothermal Methods," ASTM International, West Conshohocken, PA, 2008, DOI: 10.1520/E2070-08, www.astm.org.

[38] ASTM Standard E200, 2008, "Standard Practice for Preparation, Standardization, and Storage of Standard and Reagent Solutions for Chemical Analysis", ASTM International, West Conshohocken, PA, 2008, DOI: 10.1520/E0200-08, www.astm.org

[39] Wang, Y.; Liao, M.; Shu C. *J. Therm. Anal. Calorim.* 119, 2257-2267, 2015.

[40] Wang, Y.; Duh, Y.; Shu, C. *J. Therm. Anal. Calorim.* 85, 225-234, 2006.

[41] Kissinger, H. J., Res. Natl. Stand., 57, 217-221, 1956.

[42] File:Comparison of Surface Area vs Volume of Shapes.svg." *Comparison of Surface Area vs Volume of Shapes*. N.p., 14 June 2013. Web. 15 Jan. 2016. <https://commons.wikimedia.org/wiki/File:Comparison_of_surface_area_vs_volume_of_shapes.svg>.